

IFN γ induces epigenetic programming of human T-bet^{hi} B cells and promotes TLR7/8 and IL-21 induced differentiation

Esther Zumaquero¹, Sara L Stone¹, Christopher D Scharer², Scott A Jenks³, Anoma Nellore⁴, Betty Mousseau¹, Antonio Rosal-Vela¹, Davide Botta¹, John E Bradley⁵, Wojciech Wojciechowski⁶, Travis Ptacek^{1,7}, Maria I Danila⁵, Jeffrey C Edberg⁵, S Louis Bridges Jr⁵, Robert P Kimberly⁵, W Winn Chatham⁵, Trenton R Schoeb⁸, Alexander F Rosenberg^{1,9}, Jeremy M Boss², Ignacio Sanz³, Frances E Lund^{1*}

¹Department of Microbiology, The University of Alabama at Birmingham, Birmingham, United States; ²Department of Microbiology and Immunology, Division of Rheumatology, Emory University, Atlanta, United States; ³Department of Medicine, Division of Rheumatology, Emory University, Atlanta, United States; ⁴Department of Medicine, Division of Infectious Disease, The University of Alabama at Birmingham, Birmingham, United States; ⁵Department of Medicine, Division of Clinical Immunology and Rheumatology, The University of Alabama at Birmingham, Birmingham, United States; ⁶Center for Pediatric Biomedical Research, Flow Cytometry Shared Resource Laboratory, University of Rochester School of Medicine and Dentistry, Rochester, United States; ⁷Informatics Group, Center for Clinical and Translational Science, The University of Alabama at Birmingham, Birmingham, United States; ⁸Department of Genetics, Animal Resources Program, The University of Alabama at Birmingham, Birmingham, United States; ⁹The Informatics Institute, The University of Alabama at Birmingham, Birmingham, United States

*For correspondence:
flund@uab.edu

Competing interests: The authors declare that no competing interests exist.


Funding: See page 31

Received: 01 September 2018

Accepted: 10 May 2019

Published: 15 May 2019

Reviewing editor: Facundo D Batista, Ragon Institute of MGH, MIT and Harvard, United States

 Copyright Zumaquero et al. This article is distributed under the terms of the [Creative Commons Attribution License](#), which permits unrestricted use and redistribution provided that the original author and source are credited.

Abstract Although B cells expressing the IFN γ R or the IFN γ -inducible transcription factor T-bet promote autoimmunity in Systemic Lupus Erythematosus (SLE)-prone mouse models, the role for IFN γ signaling in human antibody responses is unknown. We show that elevated levels of IFN γ in SLE patients correlate with expansion of the T-bet expressing IgD^{neg}CD27^{neg}CD11c⁺CXCR5^{neg} (DN2) pre-antibody secreting cell (pre-ASC) subset. We demonstrate that naïve B cells form T-bet^{hi} pre-ASCs following stimulation with either Th1 cells or with IFN γ , IL-2, anti-Ig and TLR7/8 ligand and that IL-21 dependent ASC formation is significantly enhanced by IFN γ or IFN γ -producing T cells. IFN γ promotes ASC development by synergizing with IL-2 and TLR7/8 ligands to induce genome-wide epigenetic reprogramming of B cells, which results in increased chromatin accessibility surrounding IRF4 and BLIMP1 binding motifs and epigenetic remodeling of *IL21R* and *PRDM1* loci. Finally, we show that IFN γ signals poise B cells to differentiate by increasing their responsiveness to IL-21.

DOI: <https://doi.org/10.7554/eLife.41641.001>

Introduction

Systemic Lupus Erythematosus (SLE) is characterized by progressive dysregulation of the innate and adaptive arms of the immune system, which ultimately leads to loss of immune tolerance in B and T lymphocytes and the production of autoantibodies (Abs) by Ab-secreting B cells (ASCs)

(*Tsokos et al., 2016*). The hallmark SLE autoAbs recognize nuclear proteins and nucleic acids (*Gatto et al., 2016*), which are also ligands for TLR7 and TLR9 that are expressed by innate immune cells and B cells (*Avalos et al., 2010*). SLE autoAbs bound to their autoAgs form immune complexes, which are responsible for many of the clinical manifestations of SLE, particularly those associated with organ damage (*Gatto et al., 2016*). Consistent with the important role for B cells and ASCs in SLE pathogenesis (*Sanz, 2014*), the only new drug approved to treat SLE in decades, Belimumab, targets B cells.

Inflammatory cytokines and chemokines also contribute to SLE pathogenesis (*Apostolidis et al., 2011*). SLE patient PBMCs often exhibit a type I interferon (IFN) transcriptional signature and systemic IFN α is elevated in many patients (*Obermoser and Pascual, 2010*). It is less well appreciated that IFN γ is also increased in some SLE patients (*Csiszár et al., 2000; Harigai et al., 2008; Pollard et al., 2013*) and that a distinct IFN γ transcription signature can be detected in PBMCs from a portion of SLE patients (*Chiche et al., 2014; Welcher et al., 2015*). Interestingly, elevated serum IFN γ can be observed years before IFN α or autoAbs are detected in SLE patients and much earlier than clinical disease (*Munroe et al., 2016; Lu et al., 2016*). Consistent with these observations, B cells from SLE patients can exhibit signs of prior IFN γ exposure. For example, two IFN γ -inducible proteins, CXCR3 and T-bet, are more highly expressed by circulating B cells from SLE patients compared to healthy controls (*Harigai et al., 2008; Nicholas et al., 2008; Lit et al., 2007; Wang et al., 2018; Jenks et al., 2018*). Moreover, data from mouse SLE models show that clinical disease is dependent on B cell-specific expression of the IFN γ R and the IFN γ -induced transcription factors (TF) STAT1 (*Domeier et al., 2016; Jackson et al., 2016; Thibault et al., 2008*) and T-bet in some (*Rubtsova et al., 2017; Liu et al., 2017*) but not all (*Jackson et al., 2016; Du et al., 2019*) models. Taken together, these data suggest that IFN γ -driven inflammation may contribute to SLE B cell-driven pathophysiology.

Two interrelated populations of circulating B cells present in SLE patients, namely the CD11c^{hi} B cells, which are also called age associated B cells (ABCs) (*Karnell et al., 2017; Rubtsov et al., 2017*), and the IgD^{neg}CD27^{neg} B double negative (B_{DN}) B cells, which are often referred to as 'atypical' memory B cells (*Wei et al., 2007; Portugal et al., 2017*), are reported to express the IFN γ -inducible TF T-bet. These B cells, which may have been exposed to IFN γ at some step in their developmental process, are present in low numbers in the blood or tonsils of healthy individuals (*Ehrhardt et al., 2005*) and are reported to be expanded in chronically infected, aging and autoimmune individuals (reviewed in *Naradikian et al., 2016*), including patients with SLE (*Wang et al., 2018; Jenks et al., 2018*). The CD11c^{hi} population found in SLE patients is heterogeneous and contains CD11c-expressing IgD^{neg}CD27⁺ switched memory (B_{SW}) cells, IgD^{neg}CD27^{neg} naïve (B_N) cells and B_{DN} cells (*Wang et al., 2018*). The B_{DN} population is also heterogeneous and can be subdivided using CD11c and CXCR5 into the DN2 (CD11c^{hi}CXCR5^{neg}) subset, which express T-bet, and the DN1 (CD11c^{lo}CXCR5⁺) subset, which does not express T-bet (*Jenks et al., 2018*).

Despite extensive data showing that these overlapping populations of CD11c^{hi} B cells and B_{DN} cells are expanded in a number of human diseases (*Naradikian et al., 2016*), our understanding regarding their origin and function is incomplete. Although initial studies examining B_{DN} cells from malaria or HIV-infected individuals described these B cells as anergic (reviewed in *Portugal et al., 2017*), more recent studies reported that the CD11c-expressing IgD^{neg}CD27⁺CD21^{lo} activated B_{SW} cells from influenza vaccinated humans (*Lau et al., 2017*) and HIV infected patients (*Knox et al., 2017*), as well as the CD11c^{hi} cells from SLE patients (*Wang et al., 2018*) and the CD11c^{hi} DN2 cells from SLE patients (*Jenks et al., 2018*) possess phenotypic and molecular characteristics of pre-ASCs. Both the CD11c^{hi} B cells and the more narrowly defined DN2 subset from SLE patients differentiate into ASCs following stimulation (*Wang et al., 2018; Jenks et al., 2018*). Moreover, the T-bet^{hi} DN2 subset from SLE patients can produce autoAbs (*Jenks et al., 2018*), suggesting that these cells can potentially contribute to disease.

Since T-bet^{hi} DN2 pre-ASCs produce autoAbs and correlate with disease severity in SLE patients (*Jenks et al., 2018*), we set out to identify the signals that control the development and differentiation of this population into ASCs. Here we show that expansion of the DN2 cells in SLE patients correlates with systemic concentrations of IFN γ and IFN γ -induced cytokines. We demonstrate that activation of naïve B (B_N) cells from healthy donors or SLE patients with IFN γ -producing T cells or IFN γ +TLR7/8 and BCR ligands induces formation of a T-bet^{hi} pre-ASC population that is phenotypically, transcriptionally and functionally similar to the SLE T-bet^{hi} DN2 subset. We show that IFN γ

signals significantly augment ASC differentiation by sensitizing B_N cells to respond to BCR, IL-2 and TLR7/8 signals and by promoting global epigenetic changes in the activated B cells that lead to significantly increased chromatin accessibility surrounding binding sites for the key ASC commitment TFs, BLIMP1 and IRF4. We find IFN γ -dependent differentially accessible regions (DARs) within the *IL21R* and *PRDM1* (BLIMP1) loci and show that early IFN γ signaling promotes increased IL-21R expression and responsiveness. Finally, we observe that the key IFN γ -regulated epigenetic changes in the *in vitro* generated T-bet^{hi} B_{DN} pre-ASC subset and the molecular signals required to induce ASC development are conserved in the SLE patient DN2 cells. Collectively, these data suggest that IFN γ signals can augment ASC development and may regulate the formation of pathogenic autoreactive pre-ASCs in some SLE patients.

Results

Expansion of T-bet^{hi} DN2 cells correlates with systemic IFN γ levels in SLE patients

Recent studies from our group (Stone *et al.*, 2019) revealed that differentiation of mouse B cells activated in the presence of IFN γ -producing T cells was dependent on B cell intrinsic expression of the IFN γ R and the IFN γ -induced transcription factor (TF), T-bet. This result fit well with data from our group (Figure 1—figure supplement 1) and others (Rubtsova *et al.*, 2017; Liu *et al.*, 2017) showing that B cell intrinsic expression of T-bet is required for the development of autoAb-mediated disease in SLE mouse models and suggested that IFN γ signaling in B cells might also regulate development of ASCs from autoreactive B cells. Consistent with this possibility, we and others (Wang *et al.*, 2018; Jenks *et al.*, 2018) identified a population of circulating T-bet-expressing B cells in SLE patients, referred to as DN2 cells (Jenks *et al.*, 2018), that express high levels of T-bet and exhibit phenotypic and functional properties of pre-ASCs. Based on these data, we postulated that the T-bet^{hi} DN2 pre-ASC population that is expanded in a subset of SLE patients likely arises in response to IFN γ -dependent signals. To test this hypothesis, we first assessed whether expansion of the T-bet^{hi} DN2 pre-ASC subset in SLE patients correlated with IFN γ levels in these patients. Consistent with our prior studies using a different cohort of SLE patients (Jenks *et al.*, 2018), we observed that a subset of our SLE patients presented with an expanded population of circulating IgD^{neg}CD27^{neg} (double negative, B_{DN} cells) (Figure 1a–b) that could be subdivided into CD11c⁺CXCR5^{neg} DN2 cells and CD11c^{neg}CXCR5⁺ DN1 cells (Figure 1c). The DN2 cells, but not the DN1 cells, uniformly expressed high levels of T-bet (Figure 1d) and also expressed high levels of CD19 and FcRL5 (Figure 1—figure supplement 2a). In agreement with our prior studies, the T-bet^{hi} B_{DN} cells (gated as in Figure 1—figure supplement 2b) expressed intermediate levels of the ASC-promoting TFs, Blimp1 and IRF4 (Figure 1e–f,) and their presence correlated with anti-Smith autoAb titers in the patients (Figure 1g). Next, we measured cytokines in plasma from the SLE patients (Figure 1h–k). Consistent with our hypothesis, we observed a significant positive correlation between IFN γ , as well as the IFN γ -induced cytokines CXCL10, IL-6 and TNF α , and the frequency of T-bet^{hi} DN2 cells in these individuals (Figure 1h). These data therefore indicated that the circulating T-bet^{hi} B_{DN} cells present in our SLE patient cohort were phenotypically identical to the previously described (Jenks *et al.*, 2018) DN2 pre-ASC subset and that this pre-ASC population is most expanded in SLE patients with elevated amounts of autoAbs, IFN γ and IFN γ -driven inflammatory cytokines.

IFN γ -producing Th1 cells promote development of T-bet^{hi} B_{DN} cells and ASCs

Since IFN γ can induce T-bet expression in B cells (Stone *et al.*, 2019) and the T-bet^{hi} DN2 pre-ASCs are expanded in SLE patients with higher systemic levels of IFN γ , we predicted that the IFN γ might regulate the formation of T-bet^{hi} pre-ASCs. To test this, we developed an *in vitro* B cell/T cell mixed lymphocyte reaction (MLR) paired co-culture system (Figure 2a) containing B_N cells (purified as described in Figure 2—figure supplement 1a) purified from the peripheral blood or tonsil of one HD and highly polarized human Th1 and Th2 effectors (Zhu *et al.*, 2010), which were generated *in vitro* using purified naïve peripheral blood T cells isolated from a second unrelated HD. The Th1 cells expressed T-bet and produced IFN γ and IL-8 following restimulation while Th2 cells expressed GATA-3 and produced elevated levels of IL-4, IL-5, and IL-13 (Figure 2—figure supplement 1b–c).

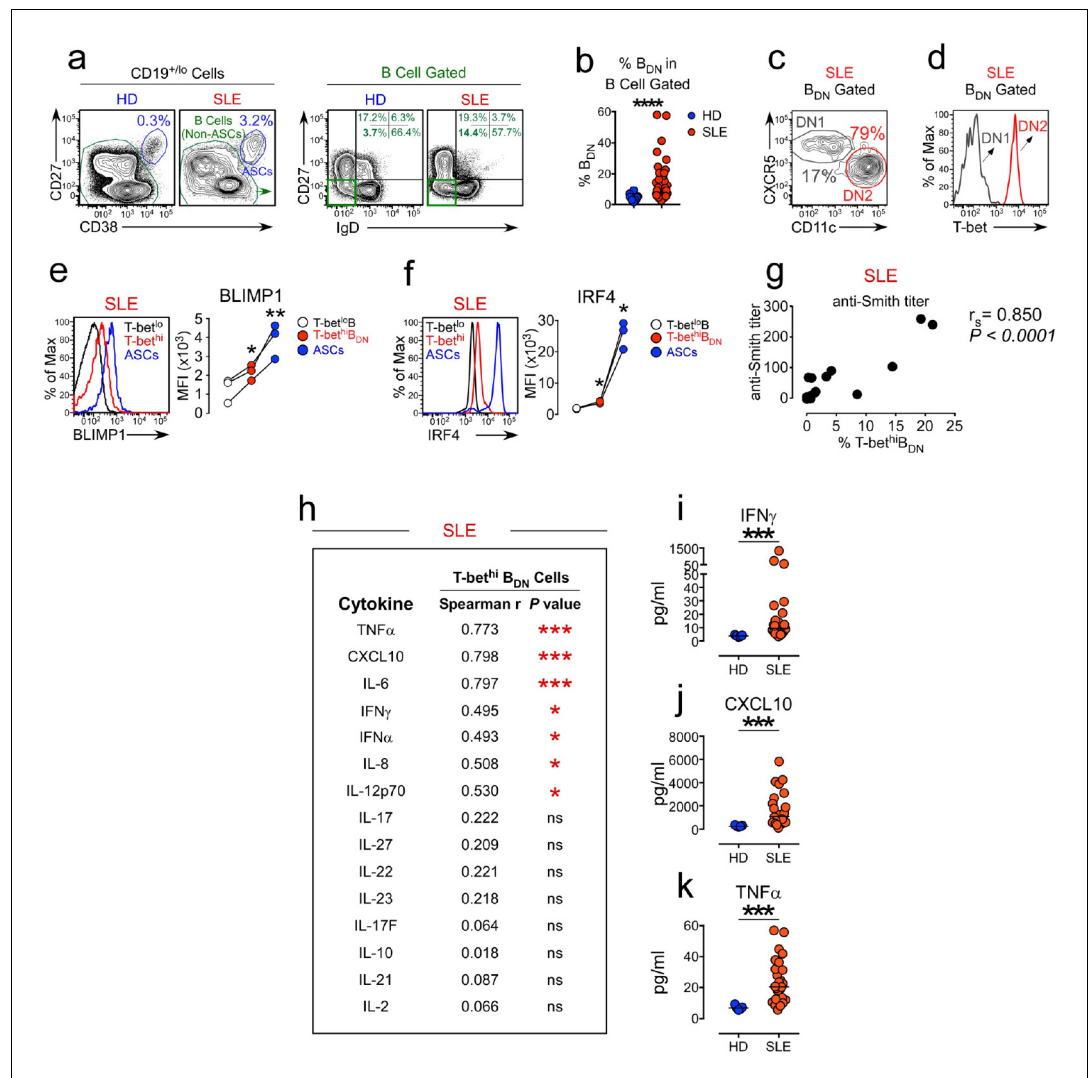


Figure 1. Expansion of the T-bet^{hi} DN2 subset in SLE patients correlates with systemic inflammatory cytokine levels. (a–f) Characterization of T-bet^{hi} B cells in peripheral blood B cell subsets from healthy donor (HD) and SLE patients. Gating strategy to identify CD38^{hi}CD27^{neg} ASCs, B cells (non-ASCs) (a, left) and double negative IgD^{neg}CD27^{neg} (B_{DN}) cells (a, right) from the peripheral blood of HD and SLE patients. Frequency of B_{DN} cells (b) within the total B cells. Subdivision of the SLE B_{DN} population into CXCR5⁺CD11c^{lo} DN1 and T-bet^{hi} CXCR5^{neg}CD11c^{hi} DN2 populations (c) with T-bet expression levels (d) in each subset shown as a histogram. Expression of BLIMP1 (e) and IRF4 (f) by ASCs, T-bet^{hi} B_{DN} cells and T-bet^{lo} B cells from SLE patients. Representative flow plots and mean fluorescence intensity (MFI) expression of BLIMP1 and IRF4 in each population are shown. (g) Correlation analysis between frequency of circulating T-bet^{hi} B_{DN} cells and anti-Smith autoAb titers in SLE patients. (h–k) Correlation (h) between plasma cytokine levels and frequency of T-bet^{hi} B_{DN} cells in SLE patient peripheral blood. Plasma concentration of IFNγ (i), CXCL10 (j) and TNFα (k) in HD (blue symbols) and SLE patients (red symbols). See **Figure 1—figure supplement 1** for analysis of T-bet expressing B cells in the Yaa. *Fcgr2b*^{-/-} SLE mouse model. See **Figure 1—figure supplement 2a** for additional phenotypic characterization of T-bet^{hi} B cells in SLE patients. See **Figure 1—figure supplement 2b** for gating strategy to identify T-bet^{hi} B_{DN} cells (DN2 cells) in SLE patients. Individual human subjects in each analysis are represented by a symbol. Horizontal black lines represent the median (b,i–k) within the group. Data shown from n = 20 HD and 40 SLE patients (b), representative flow plots from 16 SLE patients (c–d), 3 SLE patients (e–f), 16–18 SLE patients (g–h) or 5 HD and 26 SLE patients (i–k). Statistical analyses were performed using a non-parametric Mann-Whitney test (b,i–k), a one-way paired T test (e–f) or Spearman Correlation test (g–h). Correlation P and r values listed in the figure. P values *≤0.05, **<0.01, ***<0.001.

DOI: <https://doi.org/10.7554/eLife.41641.002>

The following figure supplements are available for figure 1:

Figure 1 continued on next page

Figure 1 continued

Figure supplement 1. Development of SLE in TLR7-overexpressing mice requires T-bet⁺ B cells.

DOI: <https://doi.org/10.7554/eLife.41641.003>

Figure supplement 2. Phenotypic characterization of T-bet^{hi} B cells from SLE patients.

DOI: <https://doi.org/10.7554/eLife.41641.004>

Since neither the Th1 nor Th2 cells produced IL-21 following restimulation (**Figure 2—figure supplement 1d**), we added IL-21 to the co-cultures to ensure optimal B_N activation (**Ettinger et al., 2008; Tangye, 2015**) and included IL-2 to enhance the survival of the T effectors (**Rochman et al., 2009**). After 6 days in culture, approximately 50% of the HD B cells activated in the presence of IFN γ -producing Th1 cells (Be1 cells) expressed T-bet while very few (<3%) of the HD B cells activated with IL-4 producing Th2 cells (Be2 cells) upregulated T-bet (**Figure 2b**). Approximately half of the T-bet^{hi} B cells present in the Be1 cultures downregulated IgD and these cells were CD19^{hi}CD27^{neg}CD11c⁺FcRL5⁺CD23^{neg} (**Figure 2c**). Therefore, activation of B_N cells with Th1 cells and IL-21 +IL-2 resulted in the formation of a T-bet^{hi} IgD^{neg}CD27^{neg} B_{DN} population that was phenotypically similar to the SLE patient-derived T-bet^{hi} DN2 cells.

In addition to observing the T-bet^{hi} B_{DN} pre-ASC like population in the Be1 co-cultures, we also identified CD38^{hi}CD27⁺ ASCs in both the Be1 and Be2 co-cultures (**Figure 2d**). However, we always found more ASCs in the Be1 co-cultures, even across multiple experiments using B_N and T effectors from different HD pairs (**Figure 2e**). To address whether the increased ASC formation observed in the Be1 co-cultures was limited to isotype switched or unswitched B cells, we measured the frequency of IgM and IgG-producing (gated as in **Figure 2—figure supplement 2**) ASCs across multiple paired Be1 and Be2 co-cultures. Again, we found that ASCs, regardless of isotype, were greatly enriched in the Be1 co-cultures (**Figure 2f–g**). This increase in ASCs in the Be1 co-cultures was not due to intrinsic differences in the proliferative rates of the cells in each culture but rather that a higher proportion of the Be1 cells at each cell division committed to the ASC lineage (**Figure 2—figure supplement 3**). These data indicated that Be1 co-cultures efficiently promoted the formation of T-bet^{hi} B_{DN} pre-ASC-like cells and ASCs.

T-bet^{hi} B_{DN} cells induced with Th1 cells and IL-21 are pre-ASCs

Given the phenotypic similarities between the *in vitro* generated T-bet^{hi} B_{DN} cells and SLE patient T-bet^{hi} DN2 cells and the fact that the *in vitro* cultures containing T-bet^{hi} B_{DN} cells also efficiently formed ASCs, we predicted that the *in vitro* generated Tbet^{hi} B_{DN} cells were likely to be pre-ASCs. To test this, we first asked whether the *in vitro* generated T-bet^{hi} B_{DN} cells were transcriptionally related to SLE patient-derived T-bet^{hi} DN2 pre-ASCs or to ASCs from HD. We therefore sort-purified IgD^{neg}CD27^{neg} B_{DN} cells (**Figure 3a**) from 3 independent paired day 6 Be1 and Be2 co-cultures and performed RNA-seq analysis (**Supplementary file 1**). We identified 427 differentially expressed genes (DEGs) between the B_{DN} cells from the Be1 and Be2 co-cultures (**Figure 3b**). Consistent with our data showing that T-bet was selectively upregulated in the B cells from Be1 co-cultures, we observed significantly higher levels of *TBX21* mRNA in the *in vitro* induced B_{DN} Be1 cells compared to B_{DN} Be2 cells (**Figure 3c**). Next, we used Gene Set Enrichment Analysis (GSEA) to compare the transcriptomes of the *in vitro* generated Be1 and Be2 B_{DN} cells to the T-bet^{hi} DN2 population isolated from SLE patients (**Jenks et al., 2018, Supplementary file 2**) and to curated ASC transcriptome datasets (**Abbas et al., 2005; Tarte et al., 2003**). Consistent with our phenotyping data, the transcriptome of the T-bet expressing B_{DN} Be1 cell subset was highly enriched relative to the B_{DN} Be2 cells for genes that are specifically upregulated in the SLE-derived T-bet^{hi} DN2 subset (**Figure 3d**). Moreover, the transcriptome of the *in vitro*-induced B_{DN} Be1 population was significantly enriched in expression of genes that are upregulated in ASCs compared to B_N cells (**Figure 3e**), mature B cells (**Figure 3f**) and switched memory B cells (**Figure 3g**). In addition, genes that are direct targets of IRF4 and upregulated in ASCs (**Shaffer et al., 2008**) were significantly enriched in the *in vitro* generated T-bet^{hi} Be1 B_{DN} cells relative to the Be2 B_{DN} cells (**Figure 3h**). Consistent with this finding, we observed that the Be1 T-bet^{hi} B_{DN} cells had undergone multiple rounds of cell division (**Figure 3—figure supplement 1**) and expressed intermediate levels of IRF4 (**Figure 3i–j**), when compared to the CD38^{hi}CD27⁺ ASCs and the IgD⁺CD27^{neg} B cells present in the Be1 cultures.

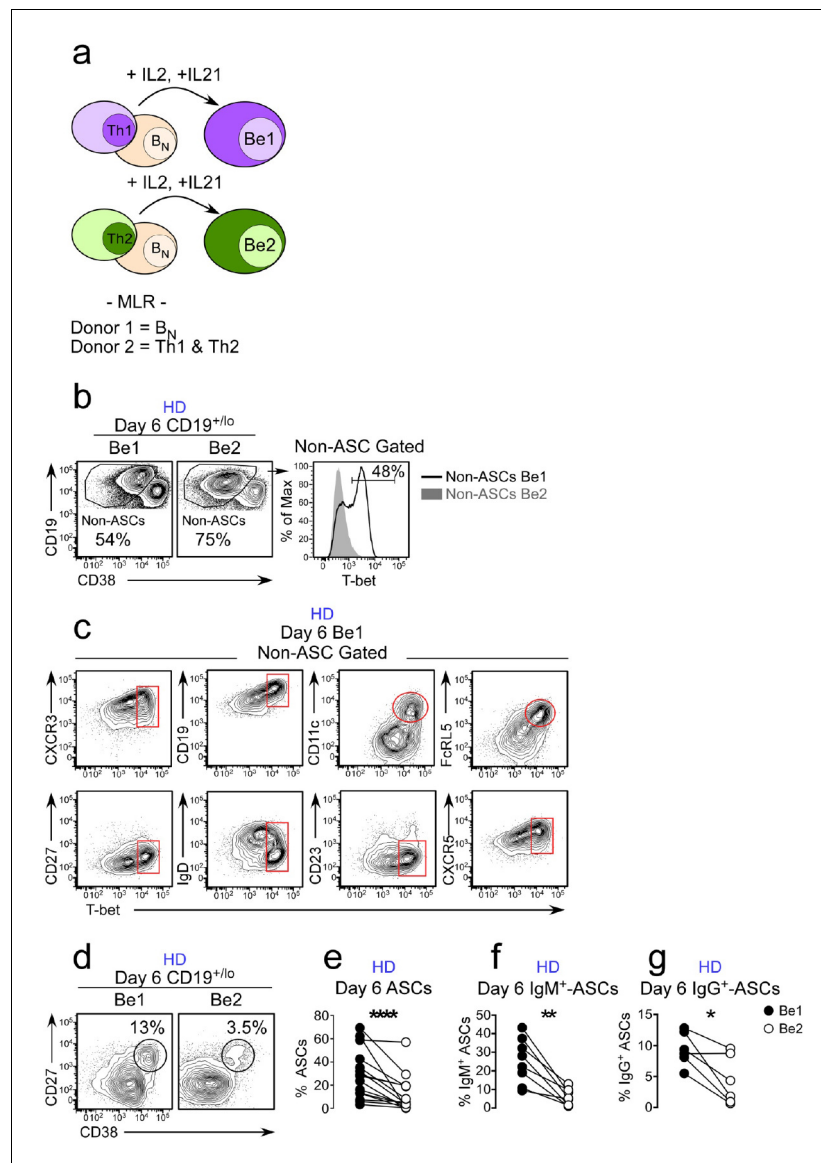


Figure 2. ASC development from B_N precursors is enhanced in Th1 containing co-cultures. Cartoon (a) depicting day 6 paired co-cultures containing Th1 (Be1 co-cultures) or Th2 (Be2 co-cultures) effectors generated from the same HD, B_N cells from a second allogeneic HD and exogenous IL-21 and IL-2. Flow cytometric analysis showing T-bet expression (b) on gated HD B cells (non-ASCs) from Be1 and Be2 co-cultures. Phenotyping (c) of day 6 B cell-gated Be1 cells showing T-bet expression in combination with other surface markers. (d–g) ASC development in HD day 6 paired Be1 and Be2 co-cultures showing representative flow plots (d) and frequencies (e) of $CD38^{hi}CD27^+$ ASCs in $CD19^{+/lo}$ -gated B lineage cells. Frequencies of IgM^+ (f) or IgG^+ (g) ASCs in day 6 paired Be1 and Be2 co-cultures. See **Figure 2—figure supplement 1** for B_N isolation strategy and characterization of polarized Th1 and Th2 effectors. See **Figure 2—figure supplement 2** for gating strategy to identify IgG^+ and IgM^+ ASCs. See **Figure 2—figure supplement 3** for proliferation analysis of B cells in paired day 6 HD Be1 and Be2 co-cultures. Analyses in (b–c) are from representative co-cultures ($n > 30$). Experiments (e–g) performed on 15 (e), 8 (f) or 6 (g) independent paired Be1 and Be2 co-cultures. Statistical analyses were performed using a non-parametric Wilcoxon paired t test (e) or paired Student's t test (f–g). P values * <0.05 , ** <0.01 , **** <0.0001 . DOI: <https://doi.org/10.7554/eLife.41641.005>

The following figure supplements are available for figure 2:

Figure supplement 1. Identification of B_N cells and characterization of *in vitro* generated Th1 and Th2 effectors.

DOI: <https://doi.org/10.7554/eLife.41641.006>

Figure supplement 2. Characterization of ASCs generated in Be1 and Be2 co-cultures.

DOI: <https://doi.org/10.7554/eLife.41641.007>

Figure 2 continued on next page

Figure 2 continued

Figure supplement 3. Proliferation analysis of B cells in paired day 6 HD Be1 and Be2 co-cultures.

DOI: <https://doi.org/10.7554/eLife.41641.008>

To determine whether the Be1 T-bet^{hi} B_{DN} cells were functional pre-ASCs, we sort-purified the IgD^{neg}CD27^{neg} B_{DN} cells from day 6 Be1 and Be2 co-cultures, labeled the sorted B_{DN} cells with Cell Trace Violet (CTV), incubated the cells for 18 hr in conditioned media and enumerated CD38^{hi}CD27⁺ ASCs in the cultures. As expected, the sorted Be1 and Be2 B_{DN} cells were activated, with 47–65% of the cells undergoing one cell division within 18 hr (**Figure 3k**). CD38^{hi}CD27⁺ ASCs were only detected in proliferating cells (**Figure 3k**), indicating that the sorted B_{DN} cells include pre-ASCs that are poised to differentiate within one round of replication. Although ASCs were detected in the cultures containing either Be1 or Be2 B_{DN} cells, significantly more ASCs were found in cultures containing the sorted T-bet expressing Be1 B_{DN} cells (**Figure 3l**). Thus, activation of B_N cells with Th1 cells and IL-21 +IL-2 gave rise to a population of T-bet^{hi} B_{DN} cells that were phenotypically, transcriptionally and functionally similar to the T-bet^{hi} DN2 pre-ASCs that are expanded in SLE patients (**Jenks et al., 2018**).

IFN γ is required for *in vitro* development of T-bet^{hi} B_{DN} pre-ASCs and ASCs from B_N cells

Since the *in vitro* generated Th1-induced T-bet^{hi} B_{DN} subset and the SLE patient derived T-bet^{hi} DN2 pre-ASC population (**Jenks et al., 2018**) were quite similar, we asked whether we could use our *in vitro* co-culture system to define the minimal signals required to generate this potentially pathogenic population of T-bet^{hi} pre-ASCs. Using Ingenuity Pathway Analysis (IPA) to interrogate the Be1 and Be2 B_{DN} cell RNA-seq data-sets, we identified predicted upstream regulators of the T-bet^{hi} B_{DN} pre-ASC transcriptional network. These included antigen receptor signaling molecules, like Btk, cytokines, like IFN α , IFN γ , IL-2 and IL-21, and cytokine-induced TFs, like STAT1 and STAT3 (**Figure 4a**). In addition, both TLR7 and TLR9 were predicted as upstream regulators of the T-bet^{hi} B_{DN} Be1 cells (**Figure 4a**). This was unexpected, given that we did not add exogenous TLR ligands to the co-cultures, however, endogenous TLR7 and TLR9 ligands are known to be released by dying cells *in vitro* (**Sindhava et al., 2017**).

Next, we addressed whether stimulation of B_N cells with the IPA-predicted activators of the T-bet^{hi} B_{DN} transcriptional network was sufficient to induce the formation of the T-bet^{hi} B_{DN} pre-ASC population. We therefore stimulated HD B_N cells with anti-Ig, cytokines (IFN γ , IL-2, IL-21 and BAFF) and the TLR7/8 ligand, R848 (**Figure 4b**) and evaluated the B cells on day 6. We found that >95% of the B_N cells activated with these defined stimuli resembled SLE patient T-bet^{hi} DN2 cells (**Jenks et al., 2018**) as the *in vitro* activated cells were IgD^{neg}CD27^{neg} T-bet^{hi}IRF4^{int}, expressed the DN2 markers, CD11c and FcRL5, and were losing expression of CD21 and CXCR5 (**Figure 4c–d**). To address which signals were critical for the *in vitro* development of T-bet^{hi} B_{DN} cells we set up ‘all minus one cultures’ by activating B_N cells for 3 days with or without individual stimuli (**Figure 4e**). As expected, when HD B_N cells were activated for 3 days in the presence of anti-Ig and all cytokines + R848 (ALL condition), essentially all of the cells upregulated T-bet and IRF4 (**Figure 4f–g**). Similar results were observed when the B_N cells were activated for 3 days without anti-Ig (**Figure 4f**) or without R848, IL-21, BAFF or IL-2 (**Figure 4g**). By contrast, when the cells were activated without IFN γ , more than 80% of the cells were T-bet^{neg/lo} (**Figure 4g**). While this wasn’t particularly surprising, given that T-bet is IFN γ -inducible (**Stone et al., 2019**), the cells also failed to upregulate IRF4 (**Figure 4g**), indicating that IFN γ signals are obligate for the *in vitro* generation of the T-bet^{hi}IRF4^{int} B_{DN} pre-ASC like population.

Although HD B_N cells activated with anti-Ig, cytokines and R848 developed in an IFN γ -dependent fashion into T-bet^{hi}IRF4^{int} B_{DN} pre-ASC like cells (**Figure 4g**), CD38^{hi}CD27⁺ ASCs did not accumulate in the cultures containing all stimuli (**Figure 4h**). This suggested that our defined cultures lacked a factor that was necessary for the differentiation of the T-bet^{hi} pre-ASC-like cells into ASCs. Alternatively, it was possible that one or more of the stimuli present in the cultures either blocked differentiation or needed to be provided transiently during a discrete temporal window. Since anti-Ig was not added in our original *in vitro* Th1 and B_N co-cultures, we first examined whether BCR signaling was

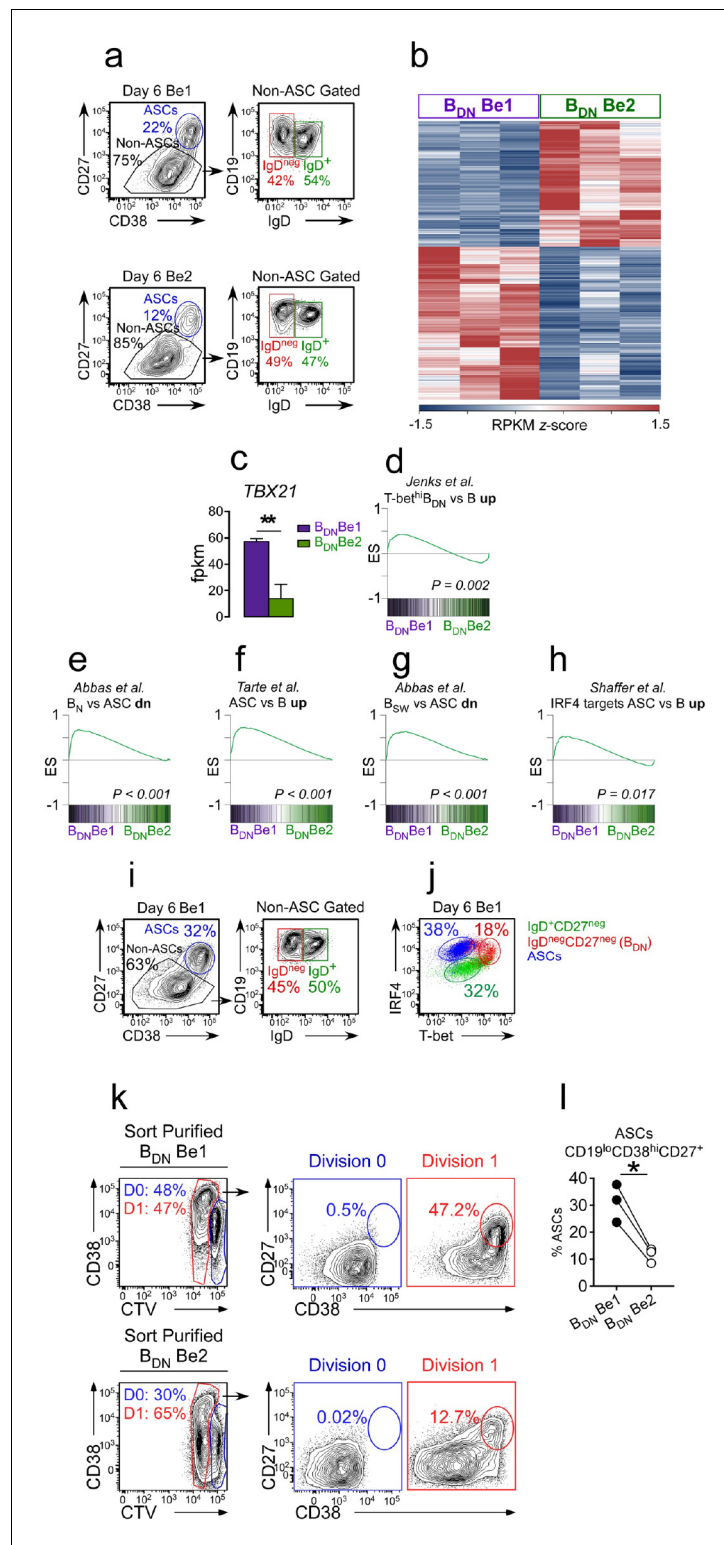


Figure 3. Th1-induced T-bet^{hi} B_{DN} cells are pre-ASCs. (a–h) Transcriptome analysis of *in vitro* generated IgD^{neg}CD27^{neg} B_{DN} cells from Be1 and Be2 co-cultures. RNA-seq analysis performed on IgD^{neg}CD27^{neg} B_{DN} cells (gating in panel a) that were sort-purified from day 6 HD Be1 and Be2 co-cultures. Heat map (b), showing 427 differentially expressed genes (DEGs) based on FDR < 0.05. T-bet mRNA expression levels (c) in B_{DN} cells from day 6 Be1 and Be2 co-cultures. Gene Set Enrichment Analysis (GSEA, panels d–h) comparing transcriptome profile of *in vitro* generated B_{DN} cells from Be1 and Be2 co-cultures with published DEGs identified in different B cell

Figure 3 continued on next page

Figure 3 continued

subsets. Data are reported as Enrichment Score (ES) plotted against the ranked B_{DN} Be1 and Be2 gene list (n = 11598). DEG lists used for GSEA include: DEGs that are upregulated in sort-purified SLE patient-derived T-bet^{hi} DN2 cells (CD19^{hi}IgD^{neg}CD27^{neg}CXCR5^{neg}IgG⁺) compared to other SLE patient-derived mature B cell subsets (d, [Jenks et al., 2018](#)); DEGs that are upregulated in human plasma cells (ASCs) relative to: B_N cells (e, [Abbas et al., 2005](#)), total B cells (f, [Tarte et al., 2003](#)) or switched memory (B_{SM}) B cells (g, [Abbas et al., 2005](#)); and IRF4-dependent upregulated target genes in ASCs (h, [Shaffer et al., 2008](#)). (i–j) IgD^{neg}CD27^{neg} T-bet^{hi} B_{DN} cells express intermediate levels of IRF4. Gating strategy (i) to identify CD38^{hi}CD27⁺ ASCs, IgD⁺CD27^{neg} B cells and IgD^{neg}CD27^{neg} B_{DN} cells in day 6 Be1 co-cultures generated from HD B_N cells. Expression of T-bet and IRF4 (j) by ASCs (blue), IgD⁺CD27^{neg} B cells (green) and IgD^{neg}CD27^{neg} B_{DN} cells (red) from day 6 Be1 co-cultures. (k–l) B_{DN} Be1 cells rapidly differentiate into ASCs. B_{DN} cells from day 6 HD Be1 and Be2 cultures were sort-purified, Cell-Trace Violet (CTV) labeled and incubated 18 hr in conditioned medium. Enumeration of ASCs (CD19^{lo}CD38^{hi}CD27⁺) in the undivided cells (D0,) and the cells that divided one time (D1,). Representative flow plots (k) showing the frequency of cells in D0 or D1 in each culture and the frequency of CD19^{lo}CD38^{hi}CD27⁺ ASCs present in the D0 or D1 fraction. Panel (l) reports frequency of ASCs within the cultures from 3 independent experiments. See [Supplementary file 1](#) for B_{DN} Be1 and Be2 RNA-seq data set and [Supplementary file 2](#) for SLE patient-derived T-bet^{hi} B_{DN} DEG list. See [Figure 3—figure supplement 1](#) for proliferation profile of the T-bet^{hi}IRF4^{int} B_{DN} subset in Be1 cells. RNA-seq performed with 3 samples/subset derived from 3 independent paired co-culture experiments. Statistical analysis performed with unpaired (c) or paired (l) Students t test. Nominal P values (d–h) for GSEA are shown. P values * < 0.05, ** < 0.01.

DOI: <https://doi.org/10.7554/eLife.41641.009>

The following figure supplement is available for figure 3:

Figure supplement 1. Comparison of the proliferative profile of T-bet^{hi}IRF4^{int} pre-ASCs and T-bet^{lo}IRF4^{hi} ASCs.

DOI: <https://doi.org/10.7554/eLife.41641.010>

blocking ASC development. We therefore stimulated B_N cells for 6 days with the complete activation cocktail (+,+) or removed the anti-Ig from the activation cocktail for the first three days (-,+), last three days (+,-), or throughout the entire culture period (-,-) ([Figure 4i](#)). Consistent with our prior results, few ASCs were recovered when anti-Ig was included throughout the culture period ([Figure 4j](#)). Similarly, excluding anti-Ig from the culture for all 6 days or for the first 3 days also resulted in poor ASC recovery ([Figure 4j](#)). However, when anti-Ig was present only during the first 3 days of culture ASCs accumulated in the cultures ([Figure 4j](#)). These data therefore argued that early but transient BCR signals were important for the development and recovery of ASCs from cytokine and R848 stimulated B_N cells.

Next, we asked whether IFN γ signals were required for the development of ASCs in the culture. We therefore activated B_N cells with the cytokine cocktail and R848 for 6 days, including 3 days in the presence of anti-Ig and 3 days without anti-Ig. In individual cultures we excluded specific cytokines or R848 for all 6 days ([Figure 4k](#)). In agreement with our earlier experiment, ASCs were recovered ([Figure 4l](#)) when B cells were transiently activated with anti-Ig in the continuous presence of R848 and the complete cytokine cocktail. Although elimination of BAFF or IL-2 from the cultures decreased the number of ASCs recovered from the cultures ([Figure 4l](#)), neither cytokine was obligate for ASC development. By contrast, and consistent with prior reports showing that ASC development from B_N cells requires IL-21 ([Ettinger et al., 2008](#); [Tangye, 2015](#)), no ASCs were detected in the cultures lacking IL-21 ([Figure 4l](#)). Likewise, ASC recovery in cultures lacking R848 or IFN γ was also at background levels ([Figure 4l](#)). Collectively, the data indicated that formation of the T-bet^{hi}IRF4^{int} pre-ASC like population required IFN γ signals while the development and recovery of ASCs were dependent on transient BCR signals, IFN γ , R848 and IL-21.

Temporal control of ASC development from T-bet^{hi}IRF4^{int} pre-ASCs by IFN γ , R848 and IL-21

Although the number of ASCs recovered from cultures lacking IL-21, R848 or IFN γ was equally low ([Figure 4l](#)), the frequencies of ASCs and number of total cells recovered from each culture differed dramatically ([Figure 4—figure supplement 1](#)). These data suggested that the different stimuli were likely to play distinct roles in the development and recovery of ASCs. Since IFN γ , but not R848 or IL-21, was required for the formation of the pre-ASC population, we postulated that IFN γ signals would be required during the initial activation (Days 0–3, priming phase) while TLR7/8 and IL-21 signals

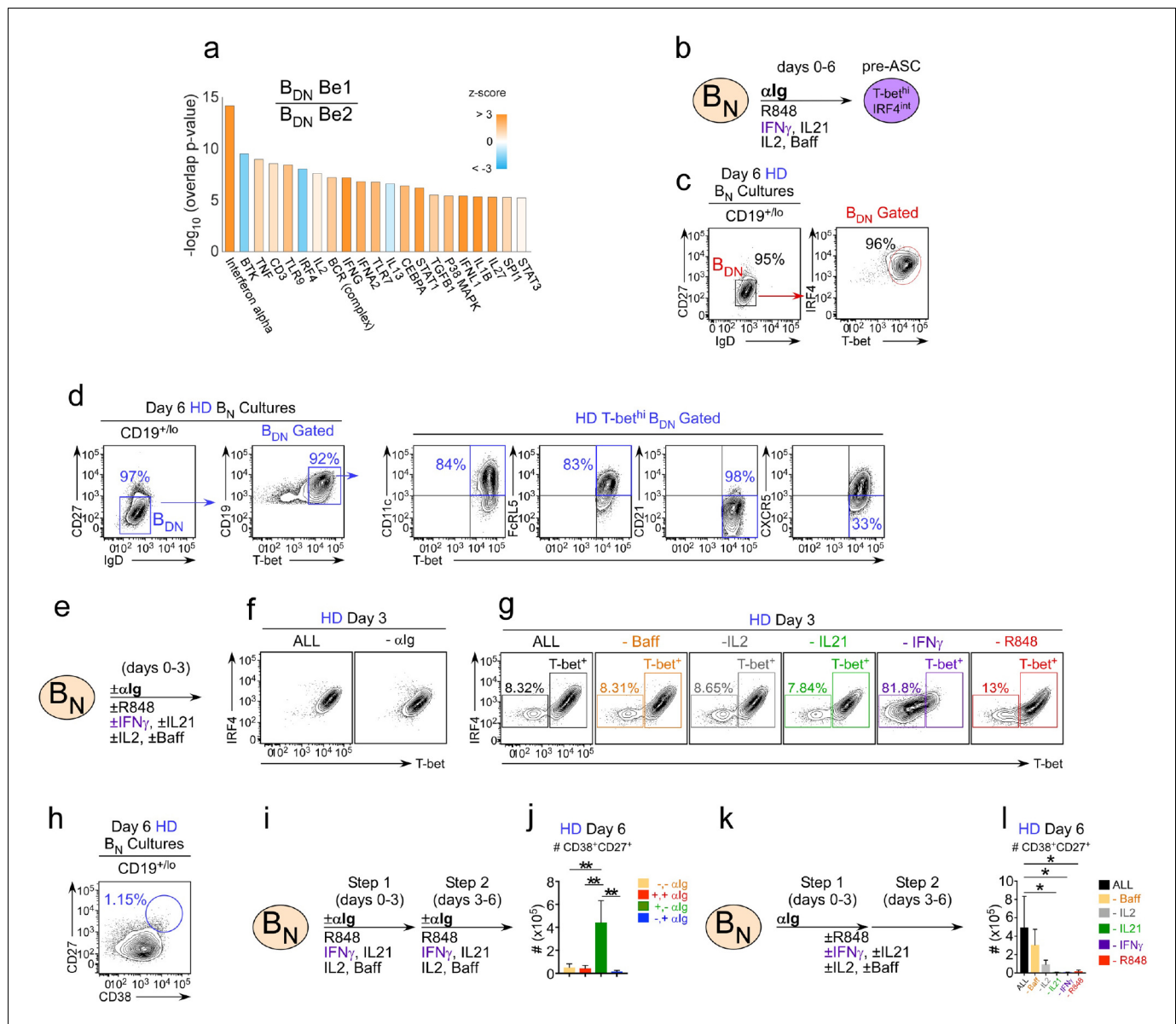


Figure 4. IFN γ is required for development of T-bet^{hi} B_{DN} cells and regulates ASC formation and recovery. (a) Ingenuity Pathway Analysis (IPA) to identify predicted upstream direct and indirect regulators of the HD B_{DN} Be1 transcriptome. IPA performed using the 427 DEG (B_{DN} Be1 over B_{DN} Be2; FDR < 0.05) identified in the RNA-seq analysis described in **Figure 3b**. The predicted activation state (z-score of B_{DN} Be1 over B_{DN} Be2) of each regulator/signaling pathway is shown as bar color (orange, activated; blue, inhibited) with predicted upstream regulators sorted in order of significance (overlap *P* value). Regulators with an overlap *P*-value < 0.00001 are shown. (b–d) IPA-identified stimuli induce development of T-bet^{hi}IRF4^{int} B_{DN} pre-ASC-like cells from HD B_{DN} cells. Cartoon (b) depicting in vitro stimulation conditions to activate purified HD B_{DN} cells with cytokines (IL-2, BAFF, IL-21, IFN γ), anti-Ig and R848 for 6 days. Phenotypic characterization of day 6 activated cells showing expression of IRF4 and T-bet (c) and other markers (d) on the IgD^{neg}CD27^{neg} B_{DN} subset. (e–h) Cartoon (e) depicting HD B_{DN} cells activated with anti-Ig + cytokine cocktail (IFN γ , IL-2, IL-21, BAFF) and R848 (ALL) or activated with individual stimuli (as indicated) removed from the cultures. Representative flow plots showing T-bet and IRF4 expression (f–g) by day 3 B cells in each culture. Enumeration of CD38^{hi}CD27⁺ ASCs (h) in day 6 ‘ALL’ cultures. (i–j) Transient BCR activation is required for ASC development. Cartoon (i) depicting activation of HD B_{DN} cells for 3 days with R848, cytokines (IFN γ , IL-2, IL-21, BAFF) \pm anti-Ig (Step 1). Cells were then washed and recultured for an additional 3 days with the same stimuli \pm anti-Ig (Step 2). Enumeration of CD38^{hi}CD27⁺ ASCs (j) on day 6 in cultures that were not exposed to anti-Ig during Steps 1 and 2 (-,-); were exposed to anti-Ig throughout Steps 1 and 2 (+,+); were exposed to anti-Ig only in Step 1 (+,-); or were exposed to anti-Ig only in Step 2 (-,+). (k–l) IFN γ , R848 and IL-21 are required for ASC development. Cartoon (k) showing HD B_{DN} cells activated with anti-Ig + cytokine cocktail (IFN γ , IL-2, IL-21, BAFF) and R848 for 3 days (Step 1) and then cultured for an additional 3 days (Step 2) with cytokine cocktail and R848. Alternatively, individual stimuli (as indicated) were excluded from the cultures for all 6 days. Enumeration of day 6 CD38^{hi}CD27⁺ ASCs (l). See **Figure 4—figure supplement 1** for % ASCs and number of total cells recovered in cultures lacking individual stimuli. RNA-seq IPA analysis was performed on n = 3 samples/subset derived from 3 independent paired co-culture experiments. Data in (c–l) are representative of ≥ 3 Figure 4 continued on next page

Figure 4 continued

experiments. The recovery of ASCs in (j, l) are shown as the mean \pm SD of cultures containing purified B_N cells from 3 independent healthy donors. Statistical analyses (j, l) were performed using one-way ANOVA with Tukey's multiple comparison test. P values * <0.05 , ** <0.01 .

DOI: <https://doi.org/10.7554/eLife.41641.011>

The following figure supplement is available for figure 4:

Figure supplement 1. IFN γ , R848 and IL-21 play distinct roles in facilitating the development and recovery of ASCs in *in vitro* cultures.

DOI: <https://doi.org/10.7554/eLife.41641.012>

would be more critical later in the culture period (Days 4–6, differentiation phase). To test this hypothesis, we activated CTV-labeled B_N cells for 3 days in the presence of anti-Ig and 3 days without anti-Ig – while adding the various stimuli minus one during the priming phase (+,-), during the differentiation phase (-,+) or throughout (+,+) the culture period (**Figure 5a**). We then measured proliferation, cell recovery and the frequency and number of ASCs present in cultures on day 6 (see **Figure 5—figure supplement 1** for representative flow cytometry plots). Eliminating IFN γ from the cultures during the first 3 days prevented formation of the T-bet^{hi}IRF4^{int} pre-ASC like population (**Figure 5—figure supplement 1a**). Moreover, consistent with our prediction, CD38^{hi}CD27⁺ ASCs, whether measured as the frequency (**Figure 5b**) or number (**Figure 5c**) were essentially undetected in cultures lacking IFN γ in the first 3 days. B_N cells that did not receive an IFN γ signal during the priming phase proliferated less over the 6 day culture period (**Figure 5d**), resulting in minimal cell recovery on day 6 (**Figure 5e**). By contrast, adding IFN γ only during the priming phase was sufficient to induce formation of the T-bet^{hi}IRF4^{int} pre-ASC population (**Figure 5—figure supplement 1a**) and to promote proliferation (**Figure 5d**) and cell recovery on day 6 (**Figure 5e**). Moreover, addition of IFN γ only during the early priming phase resulted in similar frequencies (**Figure 5b**) and numbers (**Figure 5c**) of ASCs compared to cultures that contained IFN γ throughout the entire culture period. Thus, early IFN γ signals were required to drive the development of the T-bet^{hi} pre-ASC like subset and the formation and recovery of ASCs in the cultures.

Next, we analyzed when TLR7/8 signals were necessary for ASC development. When R848 was only added during the first 3 days, ASCs could not be detected in the cultures, whether measured as the frequency (**Figure 5f**) or number (**Figure 5g**) of ASCs. This was due, at least in part, to the fact that proliferation was severely stunted (**Figure 5h**), resulting in greatly reduced cell recovery (**Figure 5i**) in the day 6 cultures. When R848 was only added to the cultures between days 3–6, we observed no impact on pre-ASC formation (**Figure 5—figure supplement 1d**) or the frequency of ASCs in the day 6 cultures (**Figure 5f**). However, the number of cells recovered on day 6 was significantly reduced (**Figure 5i**), which affected the number of ASCs recovered in the cultures (**Figure 5g**). Despite the poor recovery of cells in the cultures that received TLR7/8 stimulation only between days 3–6, proliferation of the cells was not impacted (**Figure 5h**). These data therefore indicated that R848 played both early and late roles in the development of ASCs, with early TLR7/8 signals appearing to promote B cell survival and late TLR7/8 signals promoting proliferation.

Finally, we assessed when IL-21 signals were required for ASC development. When IL-21 was only included for the first 3 days of the culture, pre-ASCs formed normally (**Figure 5—figure supplement 1g**) but ASCs could not be detected whether measured by frequency (**Figure 5j**) or number (**Figure 5k**) of ASCs recovered. The lack of ASCs in this culture correlated with greatly decreased proliferation (**Figure 5l**) and cell recovery (**Figure 5m**) on day 6. By contrast, the proliferation (**Figure 5l**) and recovery (**Figure 5m**) of cells stimulated with IL-21 only during the late phase were not significantly different from cells that were stimulated for all 6 days in the presence of IL-21. Moreover, the frequency (**Figure 5j**) and number (**Figure 5k**) of ASCs recovered from the cultures that were exposed to IL-21 between days 3–6 only were very similar to cells that were stimulated all 6 days in the presence of IL-21. Therefore, late IL-21 signals were sufficient to drive ASC formation. Thus, while inclusion of IFN γ , TLR7/8 ligand and IL-21 throughout the entire culture period promoted optimal ASC recovery, IFN γ and BCR signals were required during the priming phase, IL-21 was necessary during the later expansion and differentiation phase and R848 was important throughout the culture period (**Figure 5n**).

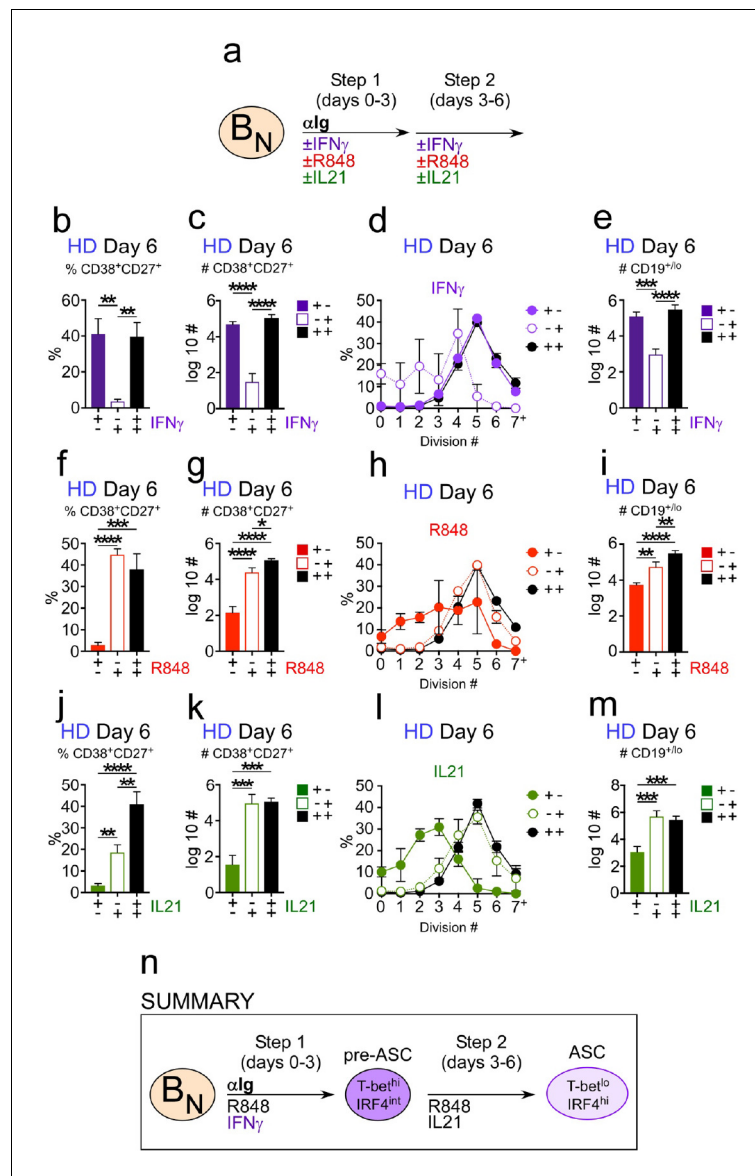


Figure 5. Temporally distinct regulation of T-bet^{hi}IRF4^{int} pre-ASC and ASC development by IFN γ , R848 and IL-21. Cartoon (a) depicting stimulation of CTV-labeled HD B_N cells for 3 days with anti-Ig, R848, IL-21 and IFN γ (Step 1). Cells were washed and re-cultured for 3 days with R848, IFN γ , and IL-21 (Step 2, +,+ condition) or individual stimuli were included in Step 1 only (+,- condition) or in Step 2 only (-,+ condition). Cells from day 6 cultures containing IFN γ (b–e), R848 (f–i) or IL-21 (j–m) in Step 1, Step 2 or both steps were analyzed to determine ASC frequencies (b, f, j), ASC recovery (c, g, k), cell division (d, h, l) and total cell recovery (e, i, m). Summary of data (n) showing that ASC development and recovery from T-bet^{hi}IRF4^{int} B_{DN} pre-ASCs requires early IFN γ , R848 and BCR ‘priming’ signals and late R848 and IL-21 proliferation and differentiation signals. See **Figure 5—figure supplement 1** for representative flow cytometry plots from each culture showing T-bet^{hi}IRF4^{int} B_{DN} cells on day 3, CD38^{hi}CD27⁺ ASCs on day 6 and CTV dilution on day 6. Data are representative of ≥ 3 experiments. The percentage of cells in each division, the frequency of ASCs and cell recovery (total and ASCs) are shown as the mean \pm SD of cultures containing purified B_N cells from 3 independent healthy donors. All statistical analyses were performed using one-way ANOVA with Tukey’s multiple comparison test. P values * <0.05 , ** <0.01 , *** <0.001 , **** <0.0001 .

DOI: <https://doi.org/10.7554/eLife.41641.013>

The following figure supplement is available for figure 5:

Figure supplement 1. Flow cytometric analysis of B cells activated during the early priming or late differentiation phase with IFN γ , R848 or IL-21.

Figure 5 continued on next page

Figure 5 continued

DOI: <https://doi.org/10.7554/eLife.41641.014>

IFN γ synergizes with R848 and IL-2 to promote proliferation, IL-21 responsiveness and ASC recovery

Our data indicated that IFN γ played a non-redundant and critical role in the formation of the Tbe-^{hi}IRF4^{int} B_{DN} cells *in vitro*, and was necessary for development and recovery of ASCs, even when IL-21 and R848 were present. These data led us to hypothesize that IFN γ signaling might sensitize B cells to respond to other stimuli, like IL-21, IL-2 and TLR ligands, that promote B cell proliferation and differentiation. To test whether IFN γ signals promoted B cell responsiveness to R848 we activated CTV-labeled HD B_N cells with anti-Ig, IL-2 and increasing concentrations of R848 in the presence and absence of IFN γ for 3 days, washed the cells and then re-cultured them for an additional 3 days with IL-21 and the same concentration of R848 that the cells were exposed to during the priming phase. On day 6 we measured cell division and ASC formation. Consistent with our earlier experiments (Figure 5), the B cells remained largely undivided when R848 was completely excluded from the cultures (Figure 6a). By contrast, when high dose R848 was included in the cultures, the cells proliferated regardless of whether IFN γ was included in the cultures for the first 3 days (Figure 6b). However, when we activated B_N cells with a 100-fold lower dose of TLR7/8 ligand, proliferation was only seen in the cultures that contained IFN γ (Figure 6c). Moreover, we observed that the frequency of ASCs in the cultures that were activated with low dose TLR ligand in the presence of IFN γ was approximately 10-fold higher than that observed for the cultures that lacked IFN γ (Figure 6d). Similar results were seen when we cross-titrated the IFN γ and R848 in the cultures (Figure 6—figure supplement 1). Thus, exposure of B_N cells to IFN γ during the initial priming phase allowed these cells to differentiate even in the face of sub-optimal stimulation with R848.

Next, we asked whether the IFN γ priming signals enhanced the early response of B cells to cytokines. We first assessed cooperation between IFN γ and IL-2 as IL-2, while not obligate for ASC development, did significantly enhance ASC recovery in our *in vitro* cultures (Figure 4). We activated HD B_N cells for 3 days with anti-Ig +R848 (Be.0 conditions), anti-Ig +R848+IL-2 (Be.IL2 conditions), anti-Ig +R848+IFN γ (Be.IFN γ conditions) or with anti-Ig +R848+IL-2+IFN γ (Be. γ 2 conditions). We then washed and stimulated the cells for an additional 3 days with R848 +IL-21 (Figure 6e) and evaluated cell recovery and ASC formation (see Figure 6—figure supplement 2 for representative flow cytometry plots). As expected, we recovered very few viable cells (Figure 6f–g) and no ASCs (Figure 6h–i) from the Be.0 cells on day 6. B cell proliferation (Figure 6f) and recovery of total cells (Figure 6g) and ASCs (Figure 6i) were also very low in the Be.IL2 cultures. Consistent with our earlier experiment (Figure 5), ASCs were easily detected in the Be.IFN γ cultures (Figure 6h–i). However, when B cells were exposed to both IL-2 and IFN γ during the early priming phase, the number of ASCs recovered on day 6 (Figure 6i) was significantly more than seen in the Be.IFN γ or Be.IL2 cultures. This was due to an increase in the number of cells recovered (Figure 6g) and to an increase in the frequency of ASCs (Figure 6h) in the cultures. Thus, early IFN γ and IL-2 signals cooperate to induce formation and recovery of ASCs.

Finally, since IL-21 signaling was obligate for ASC differentiation in our *in vitro* cultures, we hypothesized that early IFN γ signals might program the B cells to respond to IL-21. To test this hypothesis, we measured phosphorylation of the IL-21R associated TF, STAT3, before and after IL-21 stimulation in day 3 Be.0, Be.IL2, Be.IFN γ and Be. γ 2 cells. Day 3 basal levels of phospho-STAT3 were similar and low in the Be.0, Be.IL2 and Be.IFN γ cells and modestly higher in the Be. γ 2 cells (Figure 6j, see Figure 6—figure supplement 3 for flow cytometry plots). However, following a 20 min exposure to IL-21, phospho-STAT3 levels were increased significantly in the B cells that were exposed to IFN γ during the priming phase (Figure 6k), indicating that early IFN γ stimulation enhanced IL-21R signaling. Collectively, these data show that early IFN γ signals sensitize human B_N cells to respond more robustly to stimuli, like TLR7/8 ligands, IL-2 and IL-21, that promote B cell activation, proliferation and differentiation.

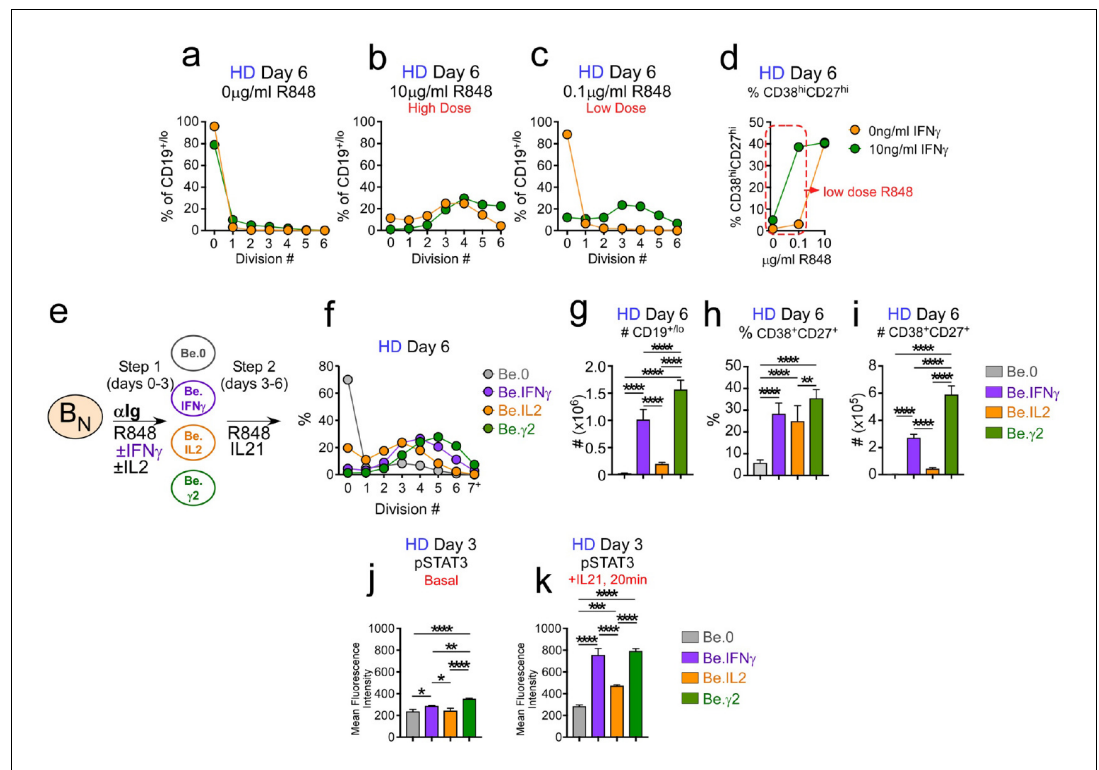


Figure 6. IFN γ cooperates with R848, IL-2 and IL-21 to promote development and recovery of ASCs. (a–d) IFN γ synergizes with subthreshold amounts of TLR7/8 ligand to induce proliferation and differentiation of B_N cells. CTV-labeled HD B_N cells were activated for 3 days (Step 1) with anti-Ig, IL-2, and increasing concentrations of R848 (as indicated) in the presence or absence of IFN γ (10 ng/ml). Cells were washed and re-cultured for 3 additional days (Step 2) with IL-21 and the same concentration of R848 that was used in Step 1. B cell division was measured on day 6 in cultures that were activated with IFN γ (green circles) or without IFN γ (orange circles) in the presence of no R848 (0 μ g/ml, (a), high dose R848 (10 μ g/ml, (b) or low dose R848 (0.1 μ g/ml, (c). The frequency of CD38^{hi}CD27⁺ ASCs (d) on day 6 is shown. (e–i) IFN γ cooperates with IL-2 to promote ASC development and recovery. Cartoon (e) depicting CTV-labeled HD B_N cells activated for 3 days (Step 1) with anti-Ig and R848 alone (Be.0); with anti-Ig +R848+IFN γ (Be.IFN γ); with anti-Ig +R848+IL-2 (Be.IL2); or with anti-Ig +R848+IFN γ +IL-2 (Be. γ 2). Cells were then washed and recultured for an additional 3 days (Step 2) with R848 and IL-21. The percentage of cells that have undergone cell division (f), the total cell recovery (g), the ASC frequencies (h) and total ASCs recovered (i) from each day 6 culture are shown. (j–k) Early IFN γ signals regulate IL-21R signaling. Phospho-STAT3 (pSTAT3) expression levels (reported as Mean Fluorescence Intensity (MFI)) in day 3 HD Be.0, Be.IFN γ , Be.IL2 and Be. γ 2 cells under basal conditions (j) or following 20 min IL-21 stimulation (k). See **Figure 6—figure supplement 1** for measurements of ASC formation in cultures containing cross-titrated IFN γ and R848. See **Figure 6—figure supplement 2** for representative flow cytometry plots from Be.0, Be.IFN γ , Be.IL2 and Be. γ 2 cells showing CD38^{hi}CD27⁺ ASCs and CTV dilution on day 6. See **Figure 6—figure supplement 3** for representative flow cytometry plots showing pSTAT3 expression. Data are representative of ≥ 3 experiments and are shown as the mean \pm SD of cultures containing purified B_N cells from 2 to 3 independent healthy donors. All statistical analyses were performed using one-way ANOVA with Tukey’s multiple comparison test. *P* values * <0.05 , ** <0.01 , *** <0.001 , **** <0.0001 .

DOI: <https://doi.org/10.7554/eLife.41641.015>

The following figure supplements are available for figure 6:

Figure supplement 1. IFN γ signals promote B cell differentiation in response to subthreshold concentrations of R848.

DOI: <https://doi.org/10.7554/eLife.41641.016>

Figure supplement 2. Flow cytometric characterization of B cells activated during the early priming phase in the presence or absence of IFN γ and IL-2.

DOI: <https://doi.org/10.7554/eLife.41641.017>

Figure supplement 3. Flow cytometric analysis of phospho-STAT3 levels in day 3 Be.0, Be.IFN γ , Be.IL2 and Be. γ 2 cells.

Figure 6 continued on next page

Figure 6 continued

DOI: <https://doi.org/10.7554/eLife.41641.018>

Early IFN γ signals cooperate with IL-2 and R848 to initiate ASC epigenetic programming and IL-21R expression

Our data showed that early IFN γ signals cooperated with both IL-2 and R848 to promote IL-21 dependent ASC formation and recovery. Given the importance of IFN γ in driving the development of the T-bet^{hi} pre-ASC like population, we hypothesized that IFN γ might induce molecular and epigenetic changes that would initiate early commitment to the ASC lineage and/or regulate IL-21R expression and responsiveness. To test this possibility, we used ATAC-seq analysis (**Supplementary file 3**) to identify differentially accessible regions (DAR) in the genome of Be.0, Be.IL2, Be.IFN γ and Be. γ 2 cells on day 3 – a time in which cell recovery was similar in the cultures (**Figure 7a–b**, see **Figure 7—figure supplement 1** for representative flow plots) and the T-bet^{hi} pre-ASC like population was easily detected in the IFN γ -containing cultures. As expected, distinct sets of DAR were found in all 4 groups of activated B cells (**Figure 7c**), however the largest number of chromatin accessible regions was seen in the day 3 Be. γ 2 cells (**Figure 7c**). Moreover, the chromatin accessibility pattern in the Be. γ 2 cells appeared to reflect cooperation or synergy between the IFN γ and IL-2 signals (**Figure 7c**). Examination of chromatin accessibility within 100 bp surrounding consensus TF binding motifs revealed significant (see **Supplementary file 4** for statistical analyses) enrichment in accessibility near T-bet binding sites in the B cells that were exposed to IFN γ (**Figure 7d**). Similarly, accessibility around STAT5 binding motifs was enriched in IL-2 exposed B cells (**Figure 7e**). However, the Be. γ 2 cells exhibited the greatest enrichment in chromatin accessibility surrounding both T-bet and STAT5 binding sites (**Figure 7d–e**), suggesting that IFN γ and IL-2 cooperate to remodel the epigenome. Consistent with this, binding motifs for NF- κ B p65 and REL, TFs activated by anti-Ig and TLR7/8 stimulation (**Kaileh and Sen, 2012**), were most accessible in the Be. γ 2 cells compared to all other groups (**Figure 7f–g**). Moreover, chromatin accessibility surrounding the HOMER-defined IRF4 and BLIMP1 binding motifs (**Heinz et al., 2010**) was also highly enriched in the Be. γ 2 cells (**Figure 7h–i**). These data therefore suggested that these key ASC initiating TFs were already exerting epigenetic changes to the genome of the Be. γ 2 cells, even before these cells were exposed to IL-21. Consistent with this finding, when we examined the *PRDM1* (BLIMP1) locus, we identified 4 DAR that were each more accessible in the Be. γ 2 cells relative to the other cells (**Figure 7j**). Although none of these DAR contained a T-bet binding motif, each DAR directly aligned with peaks previously identified in a published T-bet ChIP-seq analysis of GM12878 cells (**ENCODE Project Consortium, 2012**), suggesting that T-bet could be associated with TF complexes that bind to these regulatory regions. Moreover, 3 of the 4 *PRDM1*-associated DAR were also seen in T-bet^{hi} DN2 cells purified from SLE patients (**Figure 7j**), indicating that these DAR were present in the pre-ASC population found in SLE patients.

Finally, given our data showing that IFN γ and IL-2 potentiated signaling through the IL-21R, we examined the 2 DAR assigned to the *IL21R* locus of the day 3 cells (**Figure 7k**). One of the DAR contained two putative T-bet binding motifs and was directly aligned with a T-bet ChIP-seq peak from GM12878 cells (**ENCODE Project Consortium, 2012**) (**Figure 7k**). This DAR was only observed in the cells that were exposed to IFN γ and was most enriched in the Be. γ 2 population. Interestingly, we identified the same DAR in the SLE patient T-bet^{hi} DN2 cells (**Figure 7k**), which are reported to be highly responsive to IL-21 (**Jenks et al., 2018**). To address whether these early IFN γ -dependent epigenetic changes in the *IL21R* were associated with altered expression of IL-21R, we measured IL-21R expression in the day 3 and day 6 stimulated cells. Although day 3 B cells from Be.IFN γ and Be. γ 2 cultures expressed slightly higher levels of IL-21R compared to B cells from Be.0 and Be.IL2 cultures (**Figure 7l**), IL-21R expression were comparable between all groups at this timepoint. By day 6 however, IL-21R expression levels were 5.5–6-fold higher in the B cells that were cultured in the presence of IFN γ during the first 3 days (**Figure 7m**). Taken together, the data suggested that early IFN γ signals synergize with BCR, TLR and IL-2 signals to induce global changes in chromatin accessibility and promote increased TF binding at T-bet, NF- κ B, STAT5, BLIMP1 and IRF4 binding sites as well as chromatin remodeling at the *PRDM1* and *IL21R* loci.

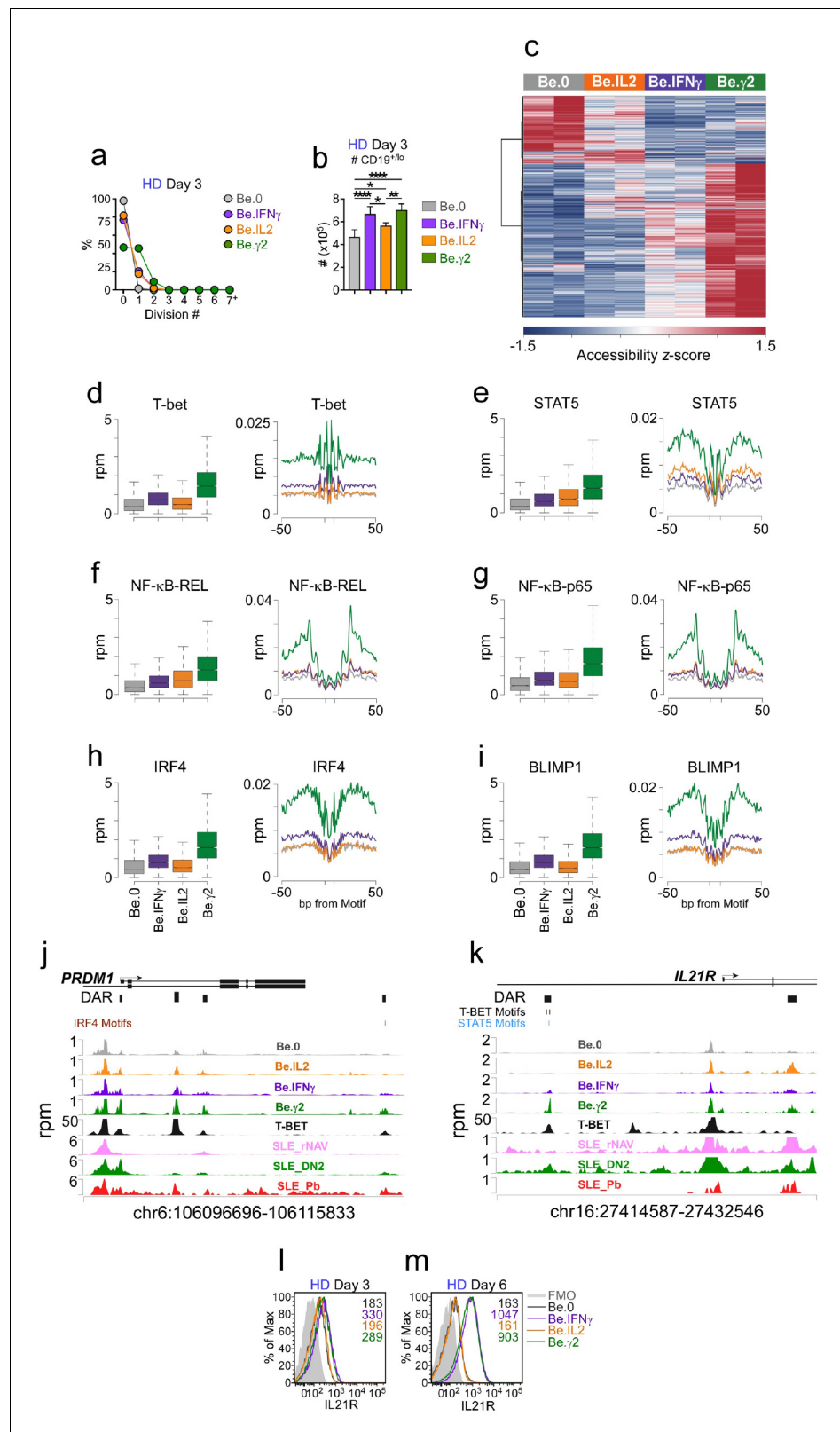


Figure 7. IFN γ signaling promotes chromatin accessibility and poises B cells to undergo IL-21 dependent differentiation. (a–b) Cell division and total cell recovery in day 3 Be.0, Be.IFN γ , Be.IL2 and Be. γ 2 cultures generated with HD B_h cells. (c–k) Chromatin accessibility analysis using ATAC-seq data from day 3 Be.0, Be.IFN γ , Be.IL2 and Be. γ 2 cell. Heatmap (c) showing 15,917 differentially accessible regions (DAR) based on FDR < 0.05. Figure 7 continued on next page

Figure 7 continued

Chromatin accessibility plots and histograms for T-bet (d), STAT5 (e), NF- κ B p65 (f), NF- κ B REL (g), IRF4 (h) and BLIMP1 (i). Plots report reads per million (rpm) in the 100 bp surrounding the transcription factor binding motifs and histograms show accessibility at the indicated motif and for the indicated surrounding sequence. Genome plots showing chromatin accessibility for the *PRMD1* (j) and *IL21R* (k) loci. DAR are shown and consensus T-bet, IRF4 and STAT5 binding motifs within DAR are indicated. DAR are aligned with previously reported T-bet binding sites in GM12878 cells (assessed by ChIP, *ENCODE Project Consortium, 2012*) and with ATAC-seq data derived from B cell subsets purified from SLE patients (*Jenks et al., 2018*). Data reported in rpm. (l–m) Early IFN γ signals control IL-21R expression levels. Representative flow plots showing IL-21R expression in day 3 (l) and day 6 (m) Be.0, Be.IFN γ , Be.IL2 and Be. γ 2 cells. See **Figure 7—figure supplement 1** for representative flow plots showing cell division profile. See **Supplementary file 3** for ATAC-seq data. See **Supplementary file 4** for enrichment of TF binding motifs *P* values. ATAC-seq analysis was performed on 3 independent experimental samples/group over 2 experiments. Flow cytometry plots depicting IL-21R expression are representative of ≥ 2 experiments. Box plots (d–i) show 1st and 3rd quartile range (box) and upper and lower range (whisker) of 2 samples/group.

DOI: <https://doi.org/10.7554/eLife.41641.019>

The following figure supplement is available for figure 7:

Figure supplement 1. Flow cytometric analysis of cell division in day 3 Be.0, Be.IFN γ , Be.IL2 and Be. γ 2 cells.

DOI: <https://doi.org/10.7554/eLife.41641.020>

SLE patient T-bet^{hi} DN2 cells differentiate into ASCs without a further requirement for BCR stimulation

Previous data from our group (*Jenks et al., 2018*) showed that the T-bet^{hi} DN2 cells from SLE patients were transcriptionally distinct from conventional memory cells and, like B_N cells (*Tan-geye, 2015*), require IL-21 signals to differentiate. Since our *in vitro* culture system accurately predicted that the T-bet^{hi} DN2 cell differentiation would be IL-21 dependent, we hypothesized that the *in vitro* culture data could be used to make additional testable predictions about the molecular properties of the T-bet^{hi} DN2 cells found in SLE patients. To evaluate this possibility, we first tested the prediction that IFN γ -dependent ASC formation from the B_N cells isolated from SLE patients would require transient BCR stimulation. We therefore purified T-bet^{lo} B_N cells (see **Figure 8—figure supplement 1** for purification strategy) from the peripheral blood of SLE patients and stimulated the cells with the complete cytokine cocktail (IFN γ , IL-2, IL-21 and BAFF) plus R848 for 6 days in the continuous presence of anti-Ig (+,+), in the complete absence of anti-Ig (-,-) or in the presence of anti-Ig for the first 3 days (+,-) (**Figure 8a**). Consistent with our prediction, SLE patient B_N cells did acquire phenotypic characteristics of the T-bet^{hi} DN2 subset following *in vitro* activation with R848, IL-2, IFN γ and IL-21 (**Figure 8b**). Moreover, the recovery of ASCs in the cultures started with SLE patient B_N cells was highly dependent on transient but early stimulation with anti-Ig as continuous stimulation with anti-Ig or no stimulation with anti-Ig reduced both the frequency and number of ASCs recovered in the cultures (**Figure 8c–d**). Thus, these data indicated that transient BCR stimulation was required for ASC development from SLE patient-derived B_N cells activated with R848, IFN γ , IL-2 and IL-21.

Based on these data and our *in vitro* experiments, we made two additional testable predictions. First, we postulated that T-bet^{hi} DN2 cells isolated from SLE patients should differentiate without a requirement for BCR stimulation. Second, we predicted that SLE patient T-bet^{hi} DN2 cells should differentiate more rapidly than B_N cells. To test these predictions, we sort-purified (see **Figure 8—figure supplement 1** for purification strategy) SLE patient-derived T-bet^{hi} DN2 cells, T-bet^{lo} B_N cells and T-bet^{lo} memory B cells, including the IgD^{neg}CD27^{neg} B_{DN} memory (DN1 cells; *Jenks et al., 2018*) and IgD^{neg}CD27⁺ memory (conventional B_{mem}) subsets. We stimulated the cells for 2.5 days with R848, IFN γ , IL-21 and IL-2 and then enumerated IgG-producing ASCs. As expected, the conventional B_{mem} and DN1 memory cells efficiently formed ASCs in this short timeframe (**Figure 8e**), while B_N cells failed to differentiate (**Figure 8e**). Consistent with our predictions, ASCs were easily identified in the day 2.5 cultures containing T-bet^{hi} DN2 cells (**Figure 8e**). Indeed, ASC recovery was at least 50-fold higher in T-bet^{hi} DN2 cell cultures compared to the B_N cultures and only 2–3 times less than that seen with the memory B cell populations (**Figure 8e**). These data therefore suggested that the expanded population of T-bet^{hi} DN2 cells present in some SLE patients likely represent a population of IFN γ , TLR ligand and antigen DN2 programmed primary effectors that can rapidly differentiate

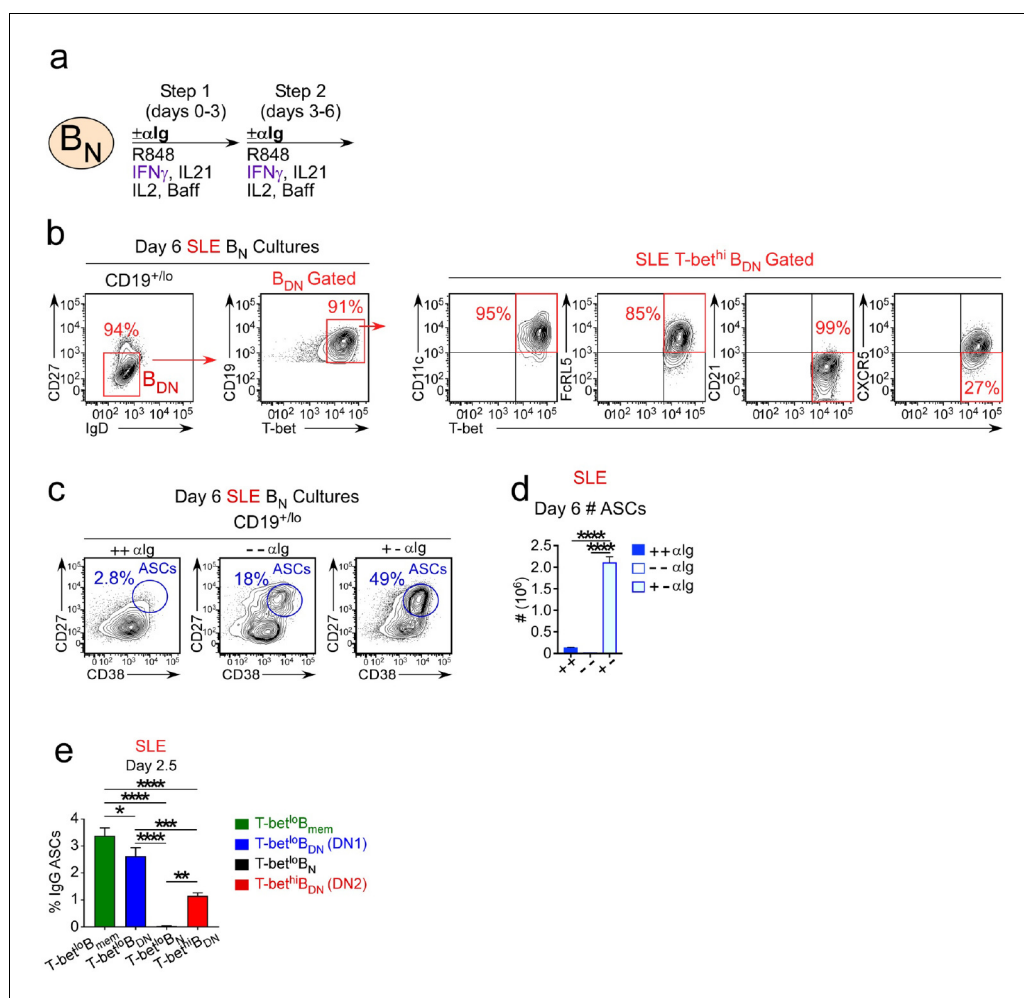


Figure 8. SLE patient T-bet^{hi} B_{DN} cells rapidly differentiate in ASCs in the absence of BCR stimulation. (a–d) ASC generation from SLE B_N cells requires early but transient BCR activation. Cartoon (a) depicting *in vitro* stimulation conditions to activate sort-purified T-bet^{lo} B_N cells from SLE patients. B_N cells were stimulated for 3 days with R848, cytokines (IFN γ , IL-2, IL-21, BAFF) \pm anti-Ig (Step 1) and then washed and recultured for an additional 3 days with the same stimuli \pm anti-Ig (Step 2). Cells were analyzed by flow cytometry on day 6 (b–d). Phenotypic characterization (b) of IgD^{neg}CD27^{neg} B_{DN} cells in cultures containing anti-Ig for all 6 days showing expression of T-bet, CD11c, FcRL5, CD21 and CXCR5 by the T-bet^{hi} B_{DN} subset. The frequency (c) and number (d) of CD38^{hi}CD27⁺ ASCs in cultures lacking anti-Ig (-,-), containing anti-Ig for all 6 days (+,+) or exposed to anti-Ig for the first 3 days only (+,-). (e) SLE patient T-bet^{hi} B_{DN} cells rapidly differentiate in ASCs. Purified SLE B cell subsets (T-bet^{lo} B_N, T-bet^{lo} CD11c^{neg}CXCR5⁺ CD27^{neg}IgD^{neg} DN1 memory cells, T-bet^{lo} CD27⁺ memory B cells (B_{mem}) and T-bet^{hi} CD11c⁺CXCR5^{neg} DN2 cells) were stimulated with cytokines (IFN γ , IL-21, IL-2, BAFF) and R848 for 2.5 days then counted and transferred to anti-IgG ELISPOT plates for 6 hr. The frequency of IgG ASCs derived from each B cell subset is shown. See **Figure 8—figure supplement 1** for gating strategy to purify B cell subsets from SLE patients. Data shown in (c–d) are from a single SLE individual and are representative of 2 independent experiments. Data reported in (e) are representative of 3 independent experiments using B cells sorted from 3 different SLE donors. Statistical analyses were performed using one-way ANOVA with Tukey’s multiple comparison test (d–e). P values * <0.05 , ** <0.01 , *** <0.001 , **** <0.0001 .

DOI: <https://doi.org/10.7554/eLife.41641.021>

The following figure supplement is available for figure 8:

Figure supplement 1. Gating strategy to sort-purify B cell subsets from SLE patients.

DOI: <https://doi.org/10.7554/eLife.41641.022>

in a BCR-signaling independent manner into ASCs following IL-21 exposure. The importance of IFN γ in driving human ASC commitment and differentiation in the context of autoimmune disease is discussed.

Discussion

Here we show that IFN γ promotes the *in vitro* formation of a T-bet^{hi}IRF4^{int} IgD^{neg}CD27^{neg} (B_{DN}) population that is similar to the T-bet expressing CD11c^{hi}CXCR5^{neg} B_{DN} (referred to as DN2 cells) subset found in SLE patients (Jenks *et al.*, 2018) and the CD11c^{hi}Age-Associated B cells (ABCs) that accumulate in aged and autoimmune mice and humans (Wang *et al.*, 2018; Rubtsov *et al.*, 2017). Both the *in vitro* generated T-bet^{hi}IRF4^{int} B_{DN} cells and SLE patient-derived DN2 cells (Jenks *et al.*, 2018) exhibit transcriptional and functional properties of pre-ASCs, suggesting that B cell intrinsic IFN γ R signals could regulate human ASC responses. While this hypothesis is supported by mouse experiments showing that IFN γ signals enhance autoAb responses (Domeier *et al.*, 2016; Jackson *et al.*, 2016; Lee *et al.*, 2012) and recent studies from our group demonstrating a role for B cell expression of the IFN γ R and the IFN γ -inducible transcription factor T-bet in ASC development (Stone *et al.*, 2019), the role for IFN γ and STAT1 signaling in human B cell differentiation is less clear. In fact, prior data showing that IFN γ has only very modest effects on activation and differentiation of human B cells (Nakagawa *et al.*, 1985; Splawski *et al.*, 1989; Rousset *et al.*, 1991) and that patients deficient in the IFN-activated transcription factor STAT1 produce Abs in response to some vaccines (Chapgier *et al.*, 2009; Chapgier *et al.*, 2006) argue that IFN γ signaling is not obligate for the formation of human ASCs. Our *in vitro* studies do not contradict this conclusion as we also find that human B cells can differentiate in the absence of IFN γ -induced signals. However, we show that B cell intrinsic IFN γ signals significantly enhance ASC differentiation induced in response to stimulation with anti-Ig, TLR7/8 ligand, IL-2 and IL-21. Indeed, we routinely recover 5- to 10 fold more ASCs in the B_N cultures that contain IFN γ or IFN γ -producing T cells compared to cultures that lack IFN γ . Thus, we argue that IFN γ signaling has the potential to augment ASC development in settings, like autoimmunity and viral infection, where IFN γ and TLR ligands are present.

Our data show that IFN γ signals, when delivered in conjunction with IL-2 and BCR +TLR7/8 ligand during the initial activation of B_N cells, greatly increase ASC recovery *in vitro*. The co-activation of B_N cells with IFN γ and IL-2 +BCR +TLR7/8 ligand results in IFN γ -dependent chromatin remodeling and the formation of the T-bet^{hi}IRF4^{int} pre-ASC subset. These early IFN γ signals are required for subsequent proliferation and differentiation following stimulation with IL-21 and TLR7/8 ligand. IFN γ is not, in and of itself, a B cell mitogen and is reported to induce apoptosis of human B cells (Bernabei *et al.*, 2001; Sammiceli *et al.*, 2011). However, we find that IFN γ synergizes with TLR7/8 ligand to promote multiple rounds of B cell proliferation – an important prerequisite of human ASC differentiation (Tangye *et al.*, 2003). Although *in vitro* experiments using human B cells show that IFN γ can synergize with TLR7 and CD40 signals to promote upregulation of Bcl6 and the acquisition of a germinal center-like phenotype (Jackson *et al.*, 2016), our data extend these studies to show that IFN γ and TLR7/8 signals also cooperate to promote human B cell differentiation. These results are analogous to studies showing that IFN α -directed signals can enhance TLR7-mediated human B cell differentiation (Jego *et al.*, 2003; Bekeredjian-Ding *et al.*, 2005). Given the considerable overlap between genes regulated by IFN α and IFN γ (Pollard *et al.*, 2013), it is possible that IFN α and IFN γ may augment TLR7 signaling in human B cells by similar mechanisms.

Our *in vitro* data suggest multiple ways in which early IFN γ priming signals promote subsequent ASC differentiation and recovery. First, we show that IFN γ cooperates with IL-2, BCR, TLR7/8 ligand to globally alter the epigenetic landscape of the activated B cells and to specifically increase chromatin accessibility surrounding NF- κ B, STAT5 and T-bet binding sites. While it is not particularly surprising that IFN γ signaling induces increased T-bet expression and alterations in chromatin accessibility around T-bet binding sites (see for example Iwata *et al.*, 2017), the finding that chromatin accessibility surrounding NF- κ B and STAT5 binding motifs is also regulated by IFN γ suggests that IFN γ must augment TLR7/8 and IL-2-dependent signaling. This is consistent with our *in vitro* data showing synergistic effects on ASC recovery when IFN γ is combined with IL-2 or R848. Second, we show that IFN γ promotes commitment to the ASC lineage by inducing expression of IRF4 and modifying chromatin accessibility surrounding IRF4-binding sites within regulatory regions in the genome of the activated B_N cells. Third, we find that IFN γ signals promote chromatin accessibility within the

PRDM1 (BLIMP1) locus and initiate chromatin remodeling around BLIMP1-binding sites within the genome of the activated B_N cells. Finally, we demonstrate that IFN γ signals alter chromatin accessibility within the *IL21R* locus of the activated B_N cells and that this change in accessibility is associated with IFN γ -dependent, increased expression of the IL-21R by the activated B_N cells and with increased responsiveness of these cells to IL-21, as measured by phosphorylation of STAT3. Collectively, these data suggest that IFN γ signals, when combined with BCR, TLR and IL-2R signals, poise human B_N cells to differentiate in response to IL-21.

One key finding from this study is that IFN γ -augmented ASC formation and recovery is highly reliant on TLR7/8 activation by its RNA and RNA/protein ligands, which are derived from viral pathogens and dead and dying cells (Avalos et al., 2010). Signaling through TLR7 is known to be important in SLE as prior studies reveal that SNPs in the human *TLR7* locus (Lee et al., 2016) and overexpression of TLR7 in mice (Pisitkun et al., 2006) are associated with increased SLE susceptibility while deletion of TLR7 protects mice from the development of SLE (Christensen et al., 2006). Our data show that deletion of the IFN γ -inducible transcription factor T-bet in B lineage cells prevents autoAb responses in a mouse model (Pisitkun et al., 2006) of TLR7-dependent SLE. Moreover, our data demonstrates that B cell intrinsic IFN γ signaling induces a TLR7/8 hyperresponsive state in human B cells. This finding does not appear to be due to IFN γ -dependent changes in the expression of TLR7 by the B cells (data not shown). Rather, we find that IFN γ -exposed B_N cells can respond and differentiate into ASCs when exposed to 100-fold lower concentration of TLR7/8 ligands than normally used to activate B cells. Given that we observed that even low levels of IFN γ are sufficient to synergize with suboptimal concentrations of TLR7/8 ligands, we predict that B cells from autoimmune patients with detectable systemic levels IFN γ will be highly sensitive to the presence of endogenous and exogenously derived TLR7 ligands.

Our data predict that TLR7-driven ASC responses are likely to be further enhanced in individuals who have increased levels of circulating IFN γ . Consistent with this, we show that SLE patients who have higher systemic levels of IFN γ also have more T-bet^{hi} DN2 cells and higher autoAb titers. We and others (Wang et al., 2018; Jenks et al., 2018) also report that the size of the T-bet^{hi} DN2 population correlates with disease activity, particularly in African-American SLE patients. However, it is important to note that T-bet^{hi} DN2 cells are unlikely to represent a purely 'pathogenic' population as we also find an inducible population of vaccine-specific T-bet^{hi} CD27^{neg} DN2 cells in healthy individuals who were immunized with inactivated influenza virus (data not shown). Similarly, others report (Lau et al., 2017; Knox et al., 2017) a T-bet expressing CD27⁺CD21^{lo} switched memory subset with pre-ASC attributes, which is induced following vaccination or infection. Thus, we speculate that the T-bet^{hi} B cells, which are found in HD and autoimmune patients in the settings of acute and chronic inflammation driven by vaccination, infection, autoimmunity and aging, are formed in an IFN γ -dependent manner and likely represent a pool of primary and secondary pre-ASCs as well as effector memory B cells that are epigenetically poised to differentiate.

The IFN γ -induced T-bet^{hi}IRF4^{int} pre-ASC population that we characterized in our *in vitro* studies is similar to the T-bet^{hi} DN2 subset that is expanded in SLE patients. Since the expansion of the T-bet^{hi} DN2 cells in SLE patients correlates with systemic levels of IFN γ and IFN γ -induced cytokines, we postulate that the DN2 cells likely arise in an IFN γ -dependent fashion in these patients. In support of this possibility, we demonstrate that the IFN γ -directed changes in chromatin accessibility within the *IL21R* and *PRDM1* loci seen in the *in vitro* generated T-bet^{hi}IRF4^{int} pre-ASCs are also found in T-bet^{hi} DN2 cells isolated from SLE patients. Moreover, we show that the molecular properties of the SLE DN2 subset and the *in vitro* generated IFN γ -dependent T-bet^{hi} B_{DN} cells are similar and unique when compared to conventional memory B cells or B_N cells. For example, as discussed above, IFN γ primes the T-bet^{hi} B_{DN} cells to respond to subthreshold concentrations of R848. Similarly, SLE DN2 cells make augmented responses to TLR7/8-stimulation compared to other B cell subsets (Jenks et al., 2018). We also show that SLE patient DN2 pre-ASCs and the *in vitro* generated T-bet^{hi} B_{DN} subset can differentiate without a need for additional BCR stimulation. This is similar to memory B cells but unlike what we find for B_N cells. However, like B_N cells (Deenick et al., 2013), both the SLE DN2 subset (Wang et al., 2018; Jenks et al., 2018) and the *in vitro* generated T-bet^{hi} B_{DN} subset require IL-21 to differentiate into ASCs. Thus, given the many shared phenotypic, molecular and functional properties of the *in vitro* generated T-bet^{hi} B_{DN} subset and the T-bet^{hi} DN2 cells found in SLE patients, we think that the *in vitro* pre-ASC cultures described here could be used to

better understand the development, maintenance and functional attributes of the T-bet^{hi} DN2 cells that are expanded and associated with more severe disease in SLE patients.

In summary, we demonstrate that IFN γ is critical for the *in vitro* formation of a T-bet^{hi}IRF4^{int} pre-ASC population that is remarkably similar to the T-bet^{hi} DN2 cells that accumulate in SLE patients who present with high autoAb titers, elevated disease activity and increased systemic levels of IFN γ . We show that IFN γ signals, particularly when combined with IL-2 and TLR7/8 + BCR ligands, initiate epigenetic reprogramming of human B cells – changes which poise the activated B_N cells to respond to IL-21 and fully commit to the ASC lineage. Based on these results, we argue that blocking IFN γ signaling in SLE patients should curtail development of T-bet^{hi} DN2 pre-ASCs from primary B_N cells, which would result in decreased autoAb production and reduced disease activity. However, results from a phase I trial examining IFN γ blockade in SLE patients did not reveal a therapeutic benefit (Boedigheimer *et al.*, 2017). Interestingly, no African Americans SLE patients with nephritis were included in the study (Boedigheimer *et al.*, 2017). Given the data showing that T-bet^{hi} DN2 cells are most expanded in African American patients with severe disease (Wang *et al.*, 2018; Jenks *et al.*, 2018) and our data presented here showing that the DN2 cells likely develop in response to IFN γ , we propose that future studies evaluating the efficacy of IFN γ blockade in SLE patients should focus specifically on the subset of patients who present with elevated IFN γ levels and significant expansion of the IFN γ -inducible T-bet expressing DN2 pre-ASC population.

Materials and methods

Key resources table

Reagent type (species) or resource	Designation	Source or reference	Identifiers	Additional information
Commercial Assays or Kits				
Commercial assay or kit	Human Anti-SM IgG ELISA Kit	Alpha Diagnostic International	3300–100-SMG	
Commercial assay or kit	Milliplex MAP Human Cytokine/Chemokine Magnetic Bead Panel	Millipore	HCYTOMAG-60K	
Commercial assay or kit	Milliplex MAP Human Th17 Magnetic Bead Panel	Millipore	HTH17MAG-14K	
Commercial assay or kit	Fixable Aqua Dead Cell Stain Kit	Life Technologies	34966	
Commercial assay or kit	CellTrace Violet	Invitrogen by Thermo Fisher Scientific	C34557	
Commercial assay or kit	Transcription Factor PhosphoPlus Buffer Set	BD Pharmingen	565575	
Commercial assay or kit	Foxp3/Transcription Factor Staining Buffer Set	eBioscience	00-5523-00	
Commercial assay or kit	EasySep Human Naïve B Cell Enrichment Set	STEMCELL Technologies	19254	
Commercial assay or kit	EasySep Human Naïve CD4 + T Cell Isolation Kit	STEMCELL Technologies	19155	
Commercial assay or kit	Anti-IgD Microbeads human	Miltenyi Biotec	130-103-775	
Commercial assay or kit	HA, Sterile Clear Plates 0.45microm Surfactant-Free, Mixed Cellulose Ester Membrane	Millipore	MAHAS4510	
Cytokines For Culture				

Continued on next page

Continued

Reagent type (species) or resource	Designation	Source or reference	Identifiers	Additional information
Peptide, recombinant protein	Recombinant Human IFN-gamma	R&D	285-IF	20 ng/ml
Peptide, recombinant protein	Recombinant Human IL4	R&D	204-IL	20 ng/ml
Peptide, recombinant protein	Recombinant Human IL12	R&D	219-IL	1 ng/ml
Peptide, recombinant protein	Recombinant Human IL21	Peprotech	200-21	10 ng/ml
Peptide, recombinant protein	Recombinant Human BAFF	Peprotech	310-13	10 ng/ml
Peptide, recombinant protein	Recombinant Human IL2	Peprotech	200-02	50 U/ml
Chemical Compounds/Drugs For Culture or Flow				
Chemical compound, drug	R848	InvivoGen	tlrl-r848	5 microgram/ml
Chemical compound, drug	Iscove's DMEM, 1X	Corning Mediatech	10-016-CV	
Chemical compound, drug	RPMI-1640	Lonza	12-702F	
Chemical compound, drug	MEM Nonessential Amino Acids	Corning Mediatech	25-025 CI	
Chemical compound, drug	Sodium Pyruvate 100 mM Solution	GE Life sciences	SH30239.01	
Chemical compound, drug	Penicillin Streptomycin Solution	Corning	30-002 CI	
Chemical compound, drug	Gentamicin	Gibco	15750-060	
Chemical compound, drug	7-amino-AMD	Calbiochem	129935	
Chemical compound, drug	Fluoresbrite Carboxylate YG 10 micron Microspheres	Polysciences	18142	
Chemical compound, drug	DPBS, 1X	Corning Mediatech	21-031-CV	
Chemical compound, drug	EDTA	Thermo Fisher Scientific	15575-038	
Chemical compound, drug	HEPES Buffer 1M Solution	Corning Mediatech	25-060 CI	
Chemical Compounds/Drugs For ELISPOT				

Continued on next page

Continued

Reagent type (species) or resource	Designation	Source or reference	Identifiers	Additional information
Chemical compound, drug	BCIP/NBT Alkaline Phosphatase Substrate/membrane	Moss, Inc	NBTM-1000	
Antibodies For Culture				
Antibody	Purified anti-human CD3 (mouse IgG1)	Biologend	300414	5 microgram/ml
Antibody	Purified anti-human CD28 (mouse IgG1)	Biologend	302914	5 microgram/ml
Antibody	Human IL-12 Antibody (goat IgG)	R&D	AB-219-NA	10 microgram/ml
Antibody	Human IFN-gamma Antibody (goat IgG)	R&D	AB-285-NA	10 microgram/ml
Antibody	Human IL-4 Antibody (goat IgG)	R&D	AB-204-NA	10 microgram/ml
Antibody	AffiniPure F(ab') ₂ Fragment Goat Anti-Human IgM, Fc μ fragment specific	Jackson ImmunoResearch	109-006-129	5 microgram/ml
Antibody	AffiniPure F(ab') ₂ Fragment Goat Anti-Human IgG, F(ab') ₂ fragment specific	Jackson ImmunoResearch	109-006-097	5 microgram/ml
Antibody	AffiniPure F(ab') ₂ Fragment Goat Anti-Human Serum IgA, α chain specific	Jackson ImmunoResearch	109-006-011	5 microgram/ml
Antibodies For ELISPOT				
Antibody	AffiniPure Goat Anti-Human IgG (H + L)	Jackson ImmunoResearch	109-005-088	2 microgram/ml
Antibody	Alkaline Phosphatase Affinipure F(ab') ₂ Fragment Goat, Anti-Human IgG, Fc-gamma Fragment Specific	Jackson ImmunoResearch	109-056-098	(1:1000)
Others For Culture				
Other	Human Serum AB	GemCell	100-512	
Other	Fetal Bovine Serum	Biowest	S1690	
Antibodies For Flow				
Antibody	Fitc Mouse Anti-Human CD3 (clone HIT3a)	BD Biosciences	555339	(1:200)
Antibody	PercP/Cy5.5 Mouse Anti-Human CD3 (clone OKT3)	eBioscience	45-0037-71	(1:200)
Antibody	Fitc Mouse Anti-Human CD4 (clone OKT4)	eBioscience	11-0048-80	(1:400)
Antibody	PE Mouse Anti-Human CD4 (clone OKT4)	Biologend	317410	(1:200)

Continued on next page

Continued

Reagent type (species) or resource	Designation	Source or reference	Identifiers	Additional information
Antibody	PercP/Cy5.5 Mouse Anti-Human CD4 (clone OKT4)	eBioscience	45-0048-42	(1:200)
Antibody	BV510 Mouse Anti-Human CD4 (clone OKT4)	Biolegend	317444	(1:100)
Antibody	Fitc Mouse Anti-Human CD11c (clone Bu15)	Biolegend	337214	(1:200)
Antibody	PE Mouse Anti-Human CD11c (clone Bu15)	Biolegend	337205	(1:400)
Antibody	PercP/Cy5.5 Mouse Anti-Human CD14 (clone HCD14)	Biolegend	325621	(1:200)
Antibody	Fitc Mouse Anti-Human CD19 (clone LT19)	Miltenyi	302256	(1:100)
Antibody	PE Mouse Anti-Human CD19 (clone HIB19)	Biolegend	302208	(1:200)
Antibody	PercP/Cy5.5 Mouse Anti-Human CD19 (clone HIB19)	Biolegend	302230	(1:100)
Antibody	APC Mouse Anti-Human CD19 (clone HIB19)	BD Pharmingen	555415	(1:200)
Antibody	APC-H7 Mouse Anti-Human CD19 (clone HIB19)	BD Pharmingen	560727	(1:100)
Antibody	BV421 Mouse Anti-Human CD19 (clone HIB19)	Biolegend	302234	(1:200)
Antibody	V500 Mouse Anti-Human CD19 (clone HIB19)	BD Horizon	561121	(1:100)
Antibody	PercP/Cy5.5 Mouse Anti-Human CD21 (clone Bu32)	Biolegend	354908	(1:100)
Antibody	Fitc Mouse Anti-Human CD23 (clone M-L23.4)	Miltenyi	130-099-365	(1:100)
Antibody	PE Mouse Anti-Human CD23 (clone EBVCS-5)	Biolegend	338507	(1:200)
Antibody	APC Mouse Anti-Human CD23 (clone M-L233)	BD Pharmingen	558690	(1:200)
Antibody	Fitc Mouse Anti-Human CD27 (clone M-T271)	Biolegend	356404	(1:100)
Antibody	PercP/Cy5.5 Mouse Anti-Human CD27 (clone M-T271)	Biolegend	356408	(1:100)
Antibody	APC Mouse Anti-Human CD27 (clone M-T271)	Biolegend	356410	(1:200)

Continued on next page

Continued

Reagent type (species) or resource	Designation	Source or reference	Identifiers	Additional information
Antibody	APC-H7 Mouse Anti-Human CD27 (clone M-T271)	eBioscience	560222	(1:100)
Antibody	BV421 Mouse Anti-Human CD27 (clone M-T271)	Biolegend	356418	(1:200)
Antibody	PE/Cy7 Mouse Anti-Human CD38 (clone HIT2)	eBioscience	25-0389-42	(1:1200)
Antibody	PercP/Cy5.5 Mouse Anti-Human CD56 (clone 5.IH11)	Biolegend	362505	(1:100)
Antibody	PE Mouse Anti-Human FcRL5 (clone 509 F6)	Biolegend	340304	(1:200)
Antibody	eFluor660 Mouse Anti-Human FcRL5 (clone 509 F6)	eBioscience	50-3078-42	(1:200)
Antibody	APC Mouse Anti-Human FcRL5 (clone 509 F6)	Biolegend	340306	(1:200)
Antibody	PE Mouse Anti-Human CXCR3 (clone CEW33D)	eBioscience	12-1839-42	(1:200)
Antibody	PE Mouse Anti-Human CXCR3 (clone 49801)	R&D	FAB160P	(1:200)
Antibody	Fitc Mouse Anti-Human CXCR5 (clone J252D4)	Biolegend	356914	(1:100)
Antibody	PE Mouse Anti-Human CXCR5 (clone J252D4)	Biolegend	356904	(1:200)
Antibody	PercP-Cy5.5 Mouse Anti-Human CXCR5 (clone J252D4)	Biolegend	356910	(1:100)
Antibody	APC Mouse Anti-Human CXCR5 (clone J252D4)	Biolegend	356907	(1:200)
Antibody	BV421 Mouse Anti-Human CXCR5 (clone J252D4)	Biolegend	356920	(1:200)
Antibody	Fitc Mouse Anti-Human IgD (clone IgD26)	Miltenyi	130-099-633	(1:100)
Antibody	Fitc Mouse Anti-Human IgD (clone IA6-2)	BD Pharmingen	555778	(1:100)
Antibody	BV421 Mouse Anti-Human IgD (clone IA6-2)	Biolegend	348226	(1:200)
Antibody	BV510 Mouse Anti-Human IgD (clone IA6-2)	BD Horizon	561490	(1:100)
Antibody	APC Mouse Anti-Human IgM (clone MHM-88)	Biolegend	314509	(1:200)

Continued on next page

Continued

Reagent type (species) or resource	Designation	Source or reference	Identifiers	Additional information
Antibody	Fitc Mouse Anti-Human IgG (clone IS11-3B2.2.3)	Miltenyi	130-099-229	(1:200)
Antibody	PE Mouse Anti-Human IgG (clone IS11-3B2.2.3)	Miltenyi	130-099-201	(1:200)
Antibody	PE Mouse Anti-Human IgA(1) (clone IS11-8E10)	Miltenyi	130-099-108	(1:200)
Antibody	PE Mouse Anti-Human IgA(2) (clone IS11-21E11)	Miltenyi	130-100-316	(1:200)
Antibody	Fitc Mouse Anti-Human/Mouse T-bet (clone 4B10)	Biolegend	644812	(1:100)
Antibody	APC Mouse Anti-Human/Mouse T-bet (clone 4B10)	Biolegend	644814	(1:100)
Antibody	AF488 Mouse Anti-Human/Mouse GATA (clone L50-823)	BD Pharmingen	560163	(1:100)
Antibody	PE Rat Anti-Human/Mouse Blimp-1 (clone 6D3)	BD Pharmingen	564702	(1:200)
Antibody	PE Rat Anti-Human/Mouse IRF4 (clone IRF4.3E4)	Biolegend	646403	(1:600)
Antibody	APC Mouse Anti-Human IL21 (clone 3A3-N2)	Biolegend	513007	(1:100)
Antibody	APC Mouse Anti-Human IL21R (clone 2 G1-K12)	Biolegend	347807	(1:50)
Antibody	BV421 Mouse Anti-Human/Mouse pSTAT3 (clone 13A3-1)	Biolegend	651009	(1:100)

Human Subjects and samples

The UAB and Emory Human Subjects Institutional Review Board approved all study protocols for HD (UAB) and SLE patients (UAB and Emory). All subjects gave written informed consent for participation and provided peripheral blood for analysis. SLE patients were recruited in collaboration with the outpatient facilities of the Division of Rheumatology and Clinical Immunology at UAB or the Division of Rheumatology at Emory. UAB and Emory SLE patients met a minimum of three ACR criteria for the classification of SLE. HDs were self-identified and recruited through the UAB Center for Clinical and Translational Science and the Alabama Vaccine Research Center (AVCR). The UAB Comprehensive Cancer Center Tissue Procurement Core Facility provided remnant tonsil tissue samples from patients undergoing routine tonsillectomies.

Lymphocyte and plasma isolation

Peripheral blood (PB) from human subjects was collected in K2-EDTA tubes (BD Bioscience). Human tonsil tissue was dissected, digested for 30 min at 37°C with DNase (150 U/ml, Sigma) and collagenase (1.25 mg/ml, Sigma), and then passed through a 70 µm cell strainer (Falcon). Human PBMCs and plasma from blood samples and low-density tonsil mononuclear cells were separated by density gradient centrifugation over Lymphocyte Separation Medium (CellGro). Red blood cells were lysed with Ammonium Chloride Solution (StemCell). Plasma was fractionated in aliquots and stored at

–80°C. Human PBMCs and tonsil mononuclear cells were either used immediately or were cryopreserved at –150°C.

Human lymphocyte purification

Naïve CD4⁺ T cells and CD19⁺ B cells were isolated from human PBMCs or tonsils using EasySep enrichment kits (StemCell). B_N cells were then positively selected using anti-IgD microbeads (Miltenyi). B cell subsets were sort-purified from PBMCs and tonsils as described in text.

Generation of Th1 and Th2 cells

Polarized CD4⁺ effector T cells were generated by activating purified HD naïve CD4 T cells with plate-bound anti-CD3 (UCHT1) and anti-CD28 (CD28.2) (both 5 µg/ml, Biolegend) in the presence of IL-2 (50 U/ml), IL-12 (1 ng/ml) and anti-IL4 (10 µg/ml) (Th1 conditions) or IL-2 (50 U/ml), IL-4 (20 ng/ml), anti-IL12 (10 µg/ml) and anti-IFNγ (10 µg/ml) (Th2 conditions). Cells were transferred into fresh media on day 3 and IL-2 was added, as needed. Cells were re-activated every 7 days using the same cultures conditions for 3 rounds of polarization. All cytokines and Abs except IL-2 (Peprotech) were purchased from R and D and T cell polarizing media contained Iscove's DMEM supplemented with penicillin (200 µg/ml), streptomycin (200 µg/ml), gentamicin (40 µg/ml), 10% FBS and 5% human serum blood type AB.

T/B co-cultures

Purified B cell subsets from HD or SLE patients were co-cultured in B cell media in the presence of IL-2 (50 U/ml)±IL-21 (10 ng/ml) with allogeneic *in vitro* generated Th1 or Th2 effectors (0.6 × 10⁶ cells/ml, ratio 5B:1T) for 5–6 days, as indicated. B cell media contained Iscove's DMEM supplemented with penicillin (200 µg/ml), streptomycin (200 µg/ml), gentamicin (40 µg/ml), 10% FBS, and insulin (5 µg/ml; Santa Cruz Biotechnology).

B cell activation with defined stimuli

Purified B cell subsets isolated from the tonsil or blood of HD or SLE patients were cultured (1 × 10⁶ cells/ml) for 3 days with 5 µg/ml anti-Ig (Jackson ImmunoResearch), 5 µg/ml R848 (InvivoGen), 50 U/ml IL-2, 10 ng/ml BAFF, 10 ng/ml IL-21 (Peprotech) and 20 ng/ml IFNγ (R and D) (Step 1). Cells were either directly analyzed or washed and recultured (2 × 10⁵ cells/ml) for an additional 3 days with the same stimuli (Step 2). The number of ASCs and total cells recovered in cultures on day 6 were determined and then normalized based on cell input. In some experiments, anti-Ig, R848, IL-21, IL-2, IFNγ or BAFF were omitted from the cultures during Step 1, or Step 2 or both steps. In other experiments, the concentration of R848 in Step 1 and Step 2 and/or the concentration of IFNγ in Step 1 was varied, as indicated in the text. In some experiments, B cell subsets isolated from blood of SLE patients and HD were stimulated for 2.5–6 days with R848 and IL-21, IL-2, BAFF and IFNγ.

STAT3 phosphorylation assays

HD B_N cells were cultured with 5 µg/ml anti-Ig and 5 µg/ml R848 alone (Be.0) or in combination with IFNγ (Be.IFNγ), IL2 (Be.IL2), or IL2 plus IFNγ (Be.γ2). On day 3 cells were washed and restimulated with medium alone or with IL-21 (10 ng/ml) for 20 min at 37°C. The cells were fixed and permeabilized with BD Transcription Factor Phospho Buffer Set and intracellular staining with anti phospho-STAT3 was performed.

In vitro B cell proliferation

Purified B cell subsets (1–5 × 10⁶ cells/ml) were stained for 10 min at 37°C with PBS diluted Cell-Trace Violet (Molecular Probes, Thermofisher). The cells were washed and either used in T effector co-culture experiments or were cultured in the presence of defined stimuli.

In vitro ASC differentiation

B_N cells were co-cultured with *in vitro* generated Th1 or Th2 cells plus IL-2 and IL-21. On day 6 of the co-culture B_{DN} cells from both cultures were sort-purified and then cultured in 0.22µM-filtered conditioned media (media collected from the original T/B co-cultures). ASCs were enumerated after 18 hr by flow cytometry.

Cytokine measurements

Th1 and Th2 cells were restimulated with platebound anti-CD3 and anti-CD28 (both 5 $\mu\text{g/ml}$). Cytokine levels in restimulated T cell cultures and SLE patient plasma samples was measured using Milliplex MAG Human Cytokine/Chemokine Immunoassays (Millipore).

Elispot

Serial diluted B cells were transferred directly to anti-IgG (Jackson ImmunoResearch) coated ELISPOT plates (Millipore) for 6 hr. Bound Ab was detected with alkaline phosphatase-conjugated anti-human IgG (Jackson ImmunoResearch) followed by development with alkaline phosphatase substrate (Moss, Inc). ELISPOTs were visualized using a CTL ELISPOT reader. The number of spots detected per well (following correction for non-specific background) was calculated.

Anti-SMITH ELISAs

Anti-Smith IgG autoantibodies in plasma from SLE patients and healthy donors were detected using the enzymatic immunoassay kit (Alpha Diagnostic) according to the manufacturer protocol.

Flow cytometry

Single cell suspensions were blocked with 10 $\mu\text{g/ml}$ FcR blocking mAb 2.4G2 (mouse cells) or with 2% human serum or human FcR blocking reagent (Miltenyi) (human cells) and then stained with fluorochrome-conjugated Abs. 7AAD or LIVE/DEAD Fixable Dead Cell Stain Kits (Molecular Probes/ThermoFisher) were used to identify live cells. For intracellular staining, cells were stained with Abs specific for cell surface markers, fixed with formalin solution (neutral buffered, 10%; Sigma) and permeabilized with 0.1% IGEPAL (Sigma) in the presence of Abs. Alternatively, the transcription factor and phospho-transcription factor staining buffers (eBioscience) were used. Stained cells were analyzed using a FACSCanto II (BD Bioscience). Cells were sort-purified with a FACSria (BD Biosciences) located in the UAB Comprehensive Flow Cytometry Core. Analysis was performed using FlowJo v9.9.3 and FlowJo v10.2.

RNA-seq library preparation and analysis

RNA samples were isolated from TRIzol (FisherThermo) treated sort-purified day 6 Be1 and Be2 IgD^{neg}CD27^{neg} B cells. 300 ng of total RNA from 3 biological replicates per B cell subset was used as input for the KAPA stranded mRNA-seq Kit with mRNA capture beads (KAPA Biosystems). Libraries were assessed for quality on a bioanalyzer, pooled, and sequenced using 50 bp paired-end chemistry on a HiSeq2500. Sequencing reads were mapped to the hg19 version of the human genome using TopHat with the default settings and the hg19 UCSC KnownGene table as a reference transcriptome. For each gene, the overlap of reads in exons was summarized using the GenomicRanges package in R/Bioconductor. Genes that contained two or more reads in at least 3 samples were deemed expressed (11598 of 23056) and used as input for edgeR to identify differentially expressed genes (DEGs). *P*-values were false-discovery rate (FDR) corrected using the Benjamini-Hochberg method and genes with a FDR of <0.05 were considered significant. Expression data was normalized to reads per kilobase per million mapped reads (FPKM). Data processing and visualization scripts are available ([Scharer, 2019a](https://github.com/elifesciences-publications/genomePlots); [Scharer, 2019b](https://github.com/elifesciences-publications/heatmap); [Scharer, 2019c](https://github.com/elifesciences-publications/plotScaledBEDfeatures); copies archived at <https://github.com/elifesciences-publications/genomePlots>, <https://github.com/elifesciences-publications/heatmap>, and <https://github.com/elifesciences-publications/plotScaledBEDfeatures> respectively). All RNA-seq data is available from the GEO database under the accession GSE95282. See also [Supplementary file 1](#).

ATAC-seq preparation and analysis

ATAC-seq data generated from the SLE B cell subsets was previously reported ([Jenks et al., 2018](#)). ATAC-seq analysis on *in vitro* generated B cell was performed on 10,000 Be.0, Be.IFN γ , Be.IL2 or Be. γ 2 cells as previously described ([Scharer et al., 2016](#)). Sorted cells were resuspended in 25 μl tagmentation reaction buffer (2.5 μl Tn5, 1x Tagment DNA Buffer, 0.2% Digitonin) and incubated for 1 hr at 37°C. Cells were lysed with 25 μl 2x Lysis Buffer (300 mM NaCl, 100 mM EDTA, 0.6% SDS, 1.6 μg Proteinase-K) for 30 min at 40°C, low molecular weight DNA was purified by size-selection with SPRI-beads (Agencourt), and then PCR amplified using Nextera primers with 2x HiFi Polymerase

Master Mix (KAPA Biosystems). Amplified, low molecular weight DNA was isolated using a second SPRI-bead size selection. Libraries were sequenced using a 50 bp paired-end run at the NYU Genome Technology Center. Raw sequencing reads were mapped to the hg19 version of the human genome using Bowtie (Langmead et al., 2009) with the default settings. Duplicate reads were marked using the Picard Tools MarkDuplicates function (<http://broadinstitute.github.io/picard/>) and eliminated from downstream analyses. Enriched accessible peaks were identified using MACS2 (Zhang et al., 2008) with the default settings. Differentially accessible regions were identified using edgeR v3.18.1 (Robinson et al., 2010) and a generalized linear model. Read counts for all peaks were annotated for each sample from the bam file using the Genomic Ranges (Lawrence et al., 2013) R/Bioconductor package and normalized to reads per million (rpm) as previously described (Scharer et al., 2016). Peaks with a greater than 2-fold change and FDR < 0.05 between comparisons were termed significant. Genomic and motif annotations were computed for ATAC-seq peaks using the HOMER (Heinz et al., 2010) annotatePeaks.pl script. The findMotifsGenome.pl function of HOMER v4.8.2 (42) was used to identify motifs enriched in DAR and the 'de novo' output was used for downstream analysis. To generate motif footprints, the motifs occurring in peaks were annotated with the HOMER v4.8.2 annotatePeaks.pl function (Heinz et al., 2010) using the options '-size given'. The read depth at the motif and surrounding sequence was computed using the GenomicRanges v1.22.4 (66) package and custom scripts in R/Bioconductor. All other analyses and data display were performed using R/Bioconductor with custom scripts (Scharer, 2019a; Scharer, 2019b; Scharer, 2019c). ATAC-seq data has been deposited in the NCBI GEO database under accession number GSE119726. See also **Supplementary files 3–5** for complete list of DAR and for analysis of TF motif enrichment in the ATAC-seq dataset.

GSEA

For gene set enrichment analysis samples were submitted to the GSEA program (<http://software.broadinstitute.org/gsea/index.jsp>). For the comparison of interest (i.e., B_{DN} Be1 and B_{DN} Be2 cells), all detected genes were ranked by multiplying the $-\log_{10}$ of the P-value from edgeR by the sign of the fold change and used as input for the GSEA Preranked analysis. The custom gene set defining genes upregulated in SLE T-bet^{hi} B_{DN} relative to other B cell subsets were derived from Jenks et al. (2018) and are listed in **Supplementary file 2**.

Ingenuity Pathway Analysis (IPA)

IPA upstream regulator analysis (Krämer et al., 2014, Qiagen, Redwood City CA) was performed using the \log_2 fold-change in gene expression between genes that were significantly differentially expressed (FDR < 0.05) in B_{DN} Be1 and B_{DN} Be2 cells. Upstream regulators with an activation z-score of ≥ 2 or ≤ -2 were considered to be activated or inhibited in B_{DN} Be1 cells. Overlap P-value (between the regulator's downstream target list and the DEG list) was based on Fisher's exact test.

Statistical analysis

Comparisons between two groups were performed with the Student's *t* test for normally distributed variables and the Mann-Whitney test for non-normally distributed variables. The one-way ANOVA test was used to compare mean values of 3 or more groups and the Kruskal-Wallis nonparametric test was used to compare medians. Strength and direction of association between two variables measures was performed using the D'Agostino-Pearson normality test followed by Pearson's or Spearman's correlation test. Data were considered significant when $p \leq 0.05$. Analysis of the data was done using the GraphPad Prism version 7.0a software (GraphPad). See **Supplementary file 5** for all statistical comparisons.

Mice and bone marrow chimeras

All experimental animals were bred and maintained in the UAB animal facilities. All procedures involving animals were approved by the UAB Institutional Animal Care and Use Committee and were conducted in accordance with the principles outlined by the National Research Council. B6.SB-Yaa/J.B6;129S-Fcgr2b^{tm1Ttk}/J (Yaa.Fcgr2b^{-/-}) (Pisitkun et al., 2006) (obtained by permission from Dr. Sylvia Bolland (NIH)) were intercrossed with B6.129S2-Ighm^{tm1Cgn}/J (μ MT) or B6.129S6-Tbx21^{tm1Glm}/J (Tbx21^{-/-}) mice (both strains obtained from Jackson Laboratory) to produce B cell deficient (Yaa.

Fcgr2b^{-/-}. μ MT) or T-bet deficient (Yaa.*Fcgr2b*^{-/-}.*Tbx21*^{-/-}) lupus-prone mice. To generate bone marrow chimeras, μ MT recipient mice were irradiated with 950 Rads from a high-energy X-ray source, delivered in a split dose 4 hr apart. Recipients were reconstituted (10^7 total BM cells) with 80% Yaa.*Fcgr2b*^{-/-}. μ MT BM +20% Yaa.*Fcgr2b*^{-/-}.*Tbx21*^{-/-} BM (B-YFT chimeras) or with 80% Yaa.*Fcgr2b*^{-/-} BM +20% Yaa.*Fcgr2b*^{-/-}.*Tbx21*^{-/-} BM (20%Control chimeras).

Mouse ANA detection and imaging

Antinuclear antibodies (ANA) were detected by an indirect immunofluorescence assay using HEp-2 cells. Fixed HEp-2-coated microscope slides (Kallestad, BioRad) were blocked, incubated with serum diluted 1:100 and stained with anti-IgG-FITC (Southern Biotech) (10 μ g/ml). Slides were mounted with SlowFade Gold Antifade Mountant with DAPI (ThermoFisher) and imaged. Anti-nuclear staining was quantitated as the mean fluorescence intensity (MFI) of IgG-FITC over DAPI-staining areas (nuclei) using NIS-Elements AR software (Nikon). Data are presented as log nuclear IgG MFI normalized by subtracting the MFI of negative control serum from B6 mice. ANA images were collected using a Nikon Eclipse Ti inverted microscope and recorded with a Clara interline CCD camera (Andor). The images were taken with a 20X (immunofluorescence) objective for 200-400X final magnification. Images were collected using NIS Elements software, scale bars were added and images were saved as high-resolution JPEGs. JPEG images were imported into Canvas Ver 12 software and were resized, cropped with the identical settings applied to all immunofluorescence images from the same experiment. Final images presented at 600–650 dpi (ANA).

Urinary Albumin to Creatinine Ratio (UACR)

Albumin concentrations in urine samples, collected from live or euthanized mice, were measured using the Mouse Albumin ELISA Quantitation Set (Bethyl Labs) according to manufacturer's protocol using a mouse reference serum as an albumin standard. To normalize for urine concentration, urinary creatinine was measured by liquid chromatography-mass spectrometry in the UAB/UCSD O'Brien Core Center for Acute Kidney Injury Research. The UACR was calculated as μ g/ml albumin divided by mg/ml creatinine and is reported as μ g albumin/mg creatinine.

Acknowledgements

We thank Thomas Scott Simpler, Uma Mudunuru, Holly Bachus, Fen Zhou, Betty Mousseau, Enid Keyser and Dr. Ji Young Hwang for technical support; Drs. Ann Marshak-Rothstein (Univ. Massachusetts), Randall Davis (UAB) and Paul Rennert for providing mice, antibodies and cell lines and Stephanie Ledbetter, Neva Gardner, Ellen Sowell and Catrena Johnson for assistance with recruitment and consenting of healthy and vaccinated subjects. We acknowledge the Tissue Procurement Facility of the NCI-supported UAB Comprehensive Cancer Center for providing remnant tonsil tissue; the Alabama Vaccine Research Clinic, the UAB RADAR biorepository and the UAB CCTS (UL1 TR001417) for assistance in procuring human samples; the UAB Animal Resources Program Comparative Pathology Laboratory for preparation of histology slides and the UAB/UCSD O'Brien Core Center for Acute Kidney Injury Research (NIH 1P30 DK 079337) for assistance with murine urine creatinine measurements. Funding for the work was provided by the US National Institutes of Health (NIH): P01 AI078907 and R01 AI110508 (to FEL), R01 AI123733 (to JMB and CDS), U19 AI109962 (to FEL and TDR), P01 AI 125180 (to IS, FEL, JMB and CDS) and R37AI049660-11 and U19 Autoimmunity Centers of Excellence AI110483 (to IS). Funding was also provided by the Lupus Research Alliance #550070 (to FEL and EZ). SLS was partially supported by the UAB Medical Scientist Training Program NIGMS T32GM008361 and MID received support from NIAMS K23 AR062100. The UAB CCTS informatics core (TP) receives support from the National Center for Advancing Translational Sciences of the National Institutes of Health under award number UL1TR001417. NIH P30 AR048311 and P30 AI027767 provided support for the UAB consolidated flow cytometry core, G2ORR022807-01 provided support for the UAB Animal Resources Program X-irradiator and 5UM1CA183728 provided funding for acquisition of human tonsil tissue.

Additional information

Funding

Funder	Grant reference number	Author
National Institutes of Health	UL1 TR001417	Travis Ptacek Jeffrey C Edberg Robert P Kimberly
National Institutes of Health	1P30 DK079337	Trenton R Schoeb
National Institutes of Health	P01 AI078907	Frances E Lund
National Institutes of Health	R01 AI110508	Frances E Lund
National Institutes of Health	R01 AI123733	Jeremy M Boss
National Institutes of Health	P01 AI125180	Jeremy M Boss Ignacio Sanz Frances E Lund
National Institutes of Health	R37 AI049660	Ignacio Sanz
National Institutes of Health	U19 AI110483	Ignacio Sanz
National Institutes of Health	T32 GM008361	Sara L Stone
National Institutes of Health	K23 AR062100	Maria I Danila
Lupus Research Alliance	#550070	Frances E Lund

The funders had no role in study design, data collection and interpretation, or the decision to submit the work for publication.

Author contributions

Esther Zumaquero, Conceptualization, Data curation, Formal analysis, Investigation, Methodology, Writing—original draft, Writing—review and editing; Sara L Stone, Conceptualization, Formal analysis, Investigation, Writing—original draft, Writing—review and editing; Christopher D Scharer, Formal analysis, Writing—review and editing; Scott A Jenks, Resources, Investigation, Writing—review and editing; Anoma Nellore, Conceptualization, Investigation, Writing—review and editing; Betty Mousseau, Formal analysis, Investigation; Antonio Rosal-Vela, Davide Botta, Investigation; John E Bradley, Resources, Methodology; Wojciech Wojciechowski, Methodology; Travis Ptacek, Data curation, Formal analysis; Maria I Danila, Jeffrey C Edberg, Robert P Kimberly, W Winn Chatham, Resources; S Louis Bridges Jr, Jeremy M Boss, Resources, Writing—review and editing; Trenton R Schoeb, Formal analysis; Alexander F Rosenberg, Data curation, Formal analysis, Visualization, Writing—review and editing; Ignacio Sanz, Conceptualization, Resources, Funding acquisition, Writing—review and editing; Frances E Lund, Conceptualization, Data curation, Formal analysis, Funding acquisition, Writing—original draft, Writing—review and editing

Author ORCIDs

Esther Zumaquero  <https://orcid.org/0000-0002-7631-7114>

Sara L Stone  <https://orcid.org/0000-0002-1689-8148>

Christopher D Scharer  <https://orcid.org/0000-0001-7716-8504>

Davide Botta  <https://orcid.org/0000-0003-3926-0662>

Frances E Lund  <https://orcid.org/0000-0003-3083-1246>

Ethics

Human subjects: All subjects gave written informed consent for participation and provided peripheral blood for analysis. The UAB and Emory Human Subjects Institutional Review Board approved all study protocols for healthy donors and SLE patients. IRB protocols 160301002, X020805006, X140213002, and N140102003 for UAB and 58515 for Emory.

Animal experimentation: All procedures involving animals were approved by the UAB Institutional Animal Care and Use Committee and were conducted in accordance with the principles outlined by the National Research Council. UAB IACUC approval IACUC-09648 and IACUC-21203.

Decision letter and Author responseDecision letter <https://doi.org/10.7554/eLife.41641.040>Author response <https://doi.org/10.7554/eLife.41641.041>**Additional files****Supplementary files**

• Supplementary file 1. RNA-seq analysis of *in vitro* generated IgD^{neg}CD27^{neg} B_{DN} Be1 and Be2 cells. RNA-seq analysis of sorted IgD^{neg}CD27^{neg} B_{DN} Be1 and Be2 cells isolated from Th1/B_N and Th2/B_N co-cultures. Data are shown as rpk values from 3 independent Be1 and Be2 co-cultures that were set up with donor-matched sets of allogeneic B_N cells and *in vitro* polarized Th1 or Th2 cells. Log₂ fold change (Be1/Be2), *P* and FDR values reported.

DOI: <https://doi.org/10.7554/eLife.41641.023>

• Supplementary file 2. Up DEG list from T-bet expressing B_{DN} cells from SLE patients. RNA-seq analysis was previously performed (Jenks *et al.*, 2018) on sort-purified T-bet^{hi}-expressing IgD^{neg}CD27^{neg}IgG⁺CXCR5^{neg} B cells from HD and SLE patients (DN2 cells). The DN2 Up DEG list is defined as genes that are significantly upregulated in SLE and HD DN2 cells relative to at least one other B cell subset (B_N, switched memory or CXCR5-expressing (T-bet^{lo}) DN1 memory = cells).

DOI: <https://doi.org/10.7554/eLife.41641.024>

• Supplementary file 3. ATAC-seq data set from day 3 Be.0, Be.IFN γ , Be.IL2 and Be. γ 2 B cell subsets. HD B_N cells were activated for 3 days with anti-Ig and R848 alone (Be.0) or in combination with: IFN γ (Be.IFN γ), IL-2 (Be.IL2) or both IFN γ +IL-2 (Be. γ 2). ATAC-seq analysis was performed on DNA isolated from each B cell subset. Table includes all identified differentially accessible regions (DAR) with fold change and FDR *q* values for each comparison. N = 2 independent samples/group.

DOI: <https://doi.org/10.7554/eLife.41641.025>

• Supplementary file 4. *P* values for ATAC-seq motif enrichment comparisons. *P* values for chromatin accessibility at transcription factor consensus DNA binding motifs (T-bet, IRF4, BLIMP1, NF-kB p65 and NF-kB REL) in ATAC-seq data. Comparisons include two-sided Student's t-test comparisons with data from day 3 Be.0, Be.IFN γ , Be.IL2 and Be. γ 2 cells.

DOI: <https://doi.org/10.7554/eLife.41641.026>

• Supplementary file 5. Complete statistical information for all data presented in this manuscript.

DOI: <https://doi.org/10.7554/eLife.41641.027>

• Transparent reporting form

DOI: <https://doi.org/10.7554/eLife.41641.028>**Data availability**

Sequencing data have been deposited in GEO under accession codes GSE95282 and GSE118984. All data generated or analyzed during this study are included in the manuscript and supporting files. Source data files for sequencing analysis are included as Supplementary Files 1 and 2 (excel files).

The following datasets were generated:

Author(s)	Year	Dataset title	Dataset URL	Database and Identifier
Lund FE, Scharer CD	2018	Chromatin accessibility of ex vivo derived Be-g2 cells	https://www.ncbi.nlm.nih.gov/geo/query/acc.cgi?acc=GSE119726	NCBI Gene Expression Omnibus, GSE119726
Lund FE, Scharer CD	2018	Be1 and Be2 B cells are transcriptionally distinct	https://www.ncbi.nlm.nih.gov/geo/query/acc.cgi?acc=GSE95282	NCBI Gene Expression Omnibus, GSE95282

The following previously published datasets were used:

Author(s)	Year	Dataset title	Dataset URL	Database and Identifier
Sanz I, Jenks S, Marigorta UM	2018	Gene expression studies of lupus and healthy B cell subsets through	https://www.ncbi.nlm.nih.gov/geo/query/acc	NCBI Gene Expression Omnibus,

References

- Abbas AR**, Baldwin D, Ma Y, Ouyang W, Gurney A, Martin F, Fong S, van Lookeren Campagne M, Godowski P, Williams PM, Chan AC, Clark HF. 2005. Immune response in silico (IRIS): immune-specific genes identified from a compendium of microarray expression data. *Genes & Immunity* **6**:319–331. DOI: <https://doi.org/10.1038/sj.gene.6364173>, PMID: 15789058
- Apostolidis SA**, Lieberman LA, Kis-Toth K, Crispin JC, Tsokos GC. 2011. The dysregulation of cytokine networks in systemic lupus erythematosus. *Journal of Interferon & Cytokine Research* **31**:769–779. DOI: <https://doi.org/10.1089/jir.2011.0029>, PMID: 21877904
- Avalos AM**, Busconi L, Marshak-Rothstein A. 2010. Regulation of autoreactive B cell responses to endogenous TLR ligands. *Autoimmunity* **43**:76–83. DOI: <https://doi.org/10.3109/08916930903374618>, PMID: 20014959
- Bekeredjian-Ding IB**, Bekeredjian-Ding IB, Wagner M, Hornung V, Giese T, Schnurr M, Endres S, Hartmann G. 2005. Plasmacytoid dendritic cells control TLR7 sensitivity of naive B cells via type I IFN. *The Journal of Immunology* **174**:4043–4050. DOI: <https://doi.org/10.4049/jimmunol.174.7.4043>, PMID: 15778362
- Bernabei P**, Coccia EM, Rigamonti L, Bosticardo M, Forni G, Pestka S, Krause CD, Battistini A, Novelli F. 2001. Interferon-gamma receptor 2 expression as the deciding factor in human T, B, and myeloid cell proliferation or death. *Journal of Leukocyte Biology* **70**:950–960. PMID: 11739558
- Boedigheimer MJ**, Martin DA, Amoura Z, Sánchez-Guerrero J, Romero-Diaz J, Kivitz A, Aranow C, Chan TM, Chong YB, Chiu K, Wang C, Sohn W, Arnold GE, Damore MA, Welcher AA, Sullivan BA, Kotzin BL, Chung JB. 2017. Safety, pharmacokinetics and pharmacodynamics of AMG 811, an anti-interferon- γ monoclonal antibody, in SLE subjects without or with lupus nephritis. *Lupus Science & Medicine* **4**:e000226. DOI: <https://doi.org/10.1136/lupus-2017-000226>, PMID: 29018537
- Chaggier A**, Wynn RF, Jouanguy E, Filipe-Santos O, Zhang S, Feinberg J, Hawkins K, Casanova JL, Arkwright PD. 2006. Human complete Stat-1 deficiency is associated with defective type I and II IFN responses *in vitro* but immunity to some low virulence viruses *in vivo*. *The Journal of Immunology* **176**:5078–5083. DOI: <https://doi.org/10.4049/jimmunol.176.8.5078>, PMID: 16585605
- Chaggier A**, Kong XF, Boisson-Dupuis S, Jouanguy E, Averbuch D, Feinberg J, Zhang SY, Bustamante J, Vogt G, Lejeune J, Mayola E, de Beaucoudrey L, Abel L, Engelhard D, Casanova JL. 2009. A partial form of recessive STAT1 deficiency in humans. *Journal of Clinical Investigation* **119**:1502–1514. DOI: <https://doi.org/10.1172/JCI37083>, PMID: 19436109
- Chiche L**, Jourde-Chiche N, Whalen E, Presnell S, Gersuk V, Dang K, Anguiano E, Quinn C, Burtey S, Berland Y, Kaplanski G, Harle JR, Pascual V, Chaussabel D. 2014. Modular transcriptional repertoire analyses of adults with systemic lupus erythematosus reveal distinct type I and type II interferon signatures. *Arthritis & Rheumatology* **66**:1583–1595. DOI: <https://doi.org/10.1002/art.38628>, PMID: 24644022
- Christensen SR**, Shupe J, Nickerson K, Kashgarian M, Flavell RA, Shlomchik MJ. 2006. Toll-like receptor 7 and TLR9 dictate autoantibody specificity and have opposing inflammatory and regulatory roles in a murine model of lupus. *Immunity* **25**:417–428. DOI: <https://doi.org/10.1016/j.immuni.2006.07.013>, PMID: 16973389
- Csiszár A**, Nagy G, Gergely P, Pozsonyi T, Pócsik E. 2000. Increased interferon-gamma (IFN-gamma), IL-10 and decreased IL-4 mRNA expression in peripheral blood mononuclear cells (PBMC) from patients with systemic lupus erythematosus (SLE). *Clinical and Experimental Immunology* **122**:464–470. DOI: <https://doi.org/10.1046/j.1365-2249.2000.01369.x>, PMID: 11122256
- Deenick EK**, Avery DT, Chan A, Berglund LJ, Ives ML, Moens L, Stoddard JL, Bustamante J, Boisson-Dupuis S, Tsumura M, Kobayashi M, Arkwright PD, Averbuch D, Engelhard D, Roesler J, Peake J, Wong M, Adelstein S, Choo S, Smart JM, et al. 2013. Naive and memory human B cells have distinct requirements for STAT3 activation to differentiate into antibody-secreting plasma cells. *The Journal of Experimental Medicine* **210**:2739–2753. DOI: <https://doi.org/10.1084/jem.20130323>, PMID: 24218138
- Domeier PP**, Chodisetti SB, Soni C, Schell SL, Elias MJ, Wong EB, Cooper TK, Kitamura D, Rahman ZS. 2016. IFN- γ receptor and STAT1 signaling in B cells are central to spontaneous germinal center formation and autoimmunity. *The Journal of Experimental Medicine* **213**:715–732. DOI: <https://doi.org/10.1084/jem.20151722>, PMID: 27069112
- Du SW**, Arkatkar T, Jacobs HM, Rawlings DJ, Jackson SW. 2019. Generation of functional murine CD11c⁺ age-associated B cells in the absence of B cell T-bet expression. *European Journal of Immunology* **49**:170–178. DOI: <https://doi.org/10.1002/eji.201847641>, PMID: 30353919
- Ehrhardt GR**, Hsu JT, Gartland L, Leu CM, Zhang S, Davis RS, Cooper MD. 2005. Expression of the immunoregulatory molecule FcRH4 defines a distinctive tissue-based population of memory B cells. *The Journal of Experimental Medicine* **202**:783–791. DOI: <https://doi.org/10.1084/jem.20050879>, PMID: 16157685
- ENCODE Project Consortium**. 2012. An integrated encyclopedia of DNA elements in the human genome. *Nature* **489**:57–74. DOI: <https://doi.org/10.1038/nature11247>, PMID: 22955616
- Ettinger R**, Kuchen S, Lipsky PE. 2008. The role of IL-21 in regulating B-cell function in health and disease. *Immunological Reviews* **223**:60–86. DOI: <https://doi.org/10.1111/j.1600-065X.2008.00631.x>, PMID: 18613830
- Gatto M**, Iaccarino L, Ghirardello A, Punzi L, Doria A. 2016. Clinical and pathologic considerations of the qualitative and quantitative aspects of lupus nephritogenic autoantibodies: a comprehensive review. *Journal of Autoimmunity* **69**:1–11. DOI: <https://doi.org/10.1016/j.jaut.2016.02.003>, PMID: 26879422

- Harigai M**, Kawamoto M, Hara M, Kubota T, Kamatani N, Miyasaka N. 2008. Excessive production of IFN- γ in patients with systemic lupus erythematosus and its contribution to induction of B lymphocyte stimulator/B cell-activating factor/TNF ligand superfamily-13B. *The Journal of Immunology* **181**:2211–2219. DOI: <https://doi.org/10.4049/jimmunol.181.3.2211>, PMID: 18641361
- Heinz S**, Benner C, Spann N, Bertolino E, Lin YC, Laslo P, Cheng JX, Murre C, Singh H, Glass CK. 2010. Simple combinations of lineage-determining transcription factors prime cis-regulatory elements required for macrophage and B cell identities. *Molecular Cell* **38**:576–589. DOI: <https://doi.org/10.1016/j.molcel.2010.05.004>, PMID: 20513432
- Iwata S**, Mikami Y, Sun HW, Brooks SR, Jankovic D, Hirahara K, Onodera A, Shih HY, Kawabe T, Jiang K, Nakayama T, Sher A, O’Shea JJ, Davis FP, Kanno Y. 2017. The transcription factor T-bet limits amplification of type I IFN transcriptome and circuitry in T helper 1 cells. *Immunity* **46**:983–991. DOI: <https://doi.org/10.1016/j.immuni.2017.05.005>, PMID: 28623086
- Jackson SW**, Jacobs HM, Arkatkar T, Dam EM, Scharping NE, Kolhatkar NS, Hou B, Buckner JH, Rawlings DJ. 2016. B cell IFN- γ receptor signaling promotes autoimmune germinal centers via cell-intrinsic induction of BCL-6. *The Journal of Experimental Medicine* **213**:733–750. DOI: <https://doi.org/10.1084/jem.20151724>, PMID: 27069113
- Jego G**, Palucka AK, Blanck JP, Chalouni C, Pascual V, Banchereau J. 2003. Plasmacytoid dendritic cells induce plasma cell differentiation through type I interferon and interleukin 6. *Immunity* **19**:225–234. DOI: [https://doi.org/10.1016/S1074-7613\(03\)00208-5](https://doi.org/10.1016/S1074-7613(03)00208-5), PMID: 12932356
- Jenks SA**, Cashman KS, Zumaquero E, Marigorta UM, Patel AV, Wang X, Tomar D, Woodruff MC, Simon Z, Bugrovsky R, Blalock EL, Scharer CD, Tipton CM, Wei C, Lim SS, Petri M, Niewold TB, Anolik JH, Gibson G, Lee FE, et al. 2018. Distinct effector B cells induced by unregulated Toll-like receptor 7 contribute to pathogenic responses in systemic lupus erythematosus. *Immunity* **49**:725–739. DOI: <https://doi.org/10.1016/j.immuni.2018.08.015>, PMID: 30314758
- Kaileh M**, Sen R. 2012. NF- κ B function in B lymphocytes. *Immunological Reviews* **246**:254–271. DOI: <https://doi.org/10.1111/j.1600-065X.2012.01106.x>, PMID: 22435560
- Karnell JL**, Kumar V, Wang J, Wang S, Voynova E, Ettinger R. 2017. Role of CD11c + T-bet + B cells in human health and disease. *Cellular Immunology* **321**:40–45. DOI: <https://doi.org/10.1016/j.cellimm.2017.05.008>
- Knox JJ**, Buggert M, Kardava L, Seaton KE, Eller MA, Canaday DH, Robb ML, Ostrowski MA, Deeks SG, Slifka MK, Tomaras GD, Moir S, Moody MA, Betts MR. 2017. T-bet+ B cells are induced by human viral infections and dominate the HIV gp140 response. *JCI Insight* **2**. DOI: <https://doi.org/10.1172/jci.insight.92943>, PMID: 28422752
- Krämer A**, Green J, Pollard J, Tugendreich S. 2014. Causal analysis approaches in ingenuity pathway analysis. *Bioinformatics* **30**:523–530. DOI: <https://doi.org/10.1093/bioinformatics/btt703>, PMID: 24336805
- Langmead B**, Trapnell C, Pop M, Salzberg SL. 2009. Ultrafast and memory-efficient alignment of short DNA sequences to the human genome. *Genome Biology* **10**:R25. DOI: <https://doi.org/10.1186/gb-2009-10-3-r25>, PMID: 19261174
- Lau D**, Lan LY, Andrews SF, Henry C, Rojas KT, Neu KE, Huang M, Huang Y, DeKosky B, Palm AE, Ippolito GC, Georgiou G, Wilson PC. 2017. Low CD21 expression defines a population of recent germinal center graduates primed for plasma cell differentiation. *Science Immunology* **2**:eaai8153. DOI: <https://doi.org/10.1126/sciimmunol.aai8153>, PMID: 28783670
- Lawrence M**, Huber W, Pagès H, Aboyoun P, Carlson M, Gentleman R, Morgan MT, Carey VJ. 2013. Software for computing and annotating genomic ranges. *PLOS Computational Biology* **9**:e1003118. DOI: <https://doi.org/10.1371/journal.pcbi.1003118>, PMID: 23950696
- Lee SK**, Silva DG, Martin JL, Pratama A, Hu X, Chang PP, Walters G, Vinuesa CG. 2012. Interferon- γ excess leads to pathogenic accumulation of follicular helper T cells and germinal centers. *Immunity* **37**:880–892. DOI: <https://doi.org/10.1016/j.immuni.2012.10.010>, PMID: 23159227
- Lee YH**, Choi SJ, Ji JD, Song GG. 2016. Association between toll-like receptor polymorphisms and systemic lupus erythematosus: a meta-analysis update. *Lupus* **25**:593–601. DOI: <https://doi.org/10.1177/0961203315622823>, PMID: 26762473
- Lit LC**, Wong CK, Li EK, Tam LS, Lam CW, Lo YM. 2007. Elevated gene expression of Th1/Th2 associated transcription factors is correlated with disease activity in patients with systemic lupus erythematosus. *The Journal of Rheumatology* **34**:89–96. PMID: 17117487
- Liu Y**, Zhou S, Qian J, Wang Y, Yu X, Dai D, Dai M, Wu L, Liao Z, Xue Z, Wang J, Hou G, Ma J, Harley JB, Tang Y, Shen N. 2017. T-bet⁺CD11c⁺ B cells are critical for antichromatin immunoglobulin G production in the development of lupus. *Arthritis Research & Therapy* **19**:225. DOI: <https://doi.org/10.1186/s13075-017-1438-2>, PMID: 28982388
- Lu R**, Munroe ME, Guthridge JM, Bean KM, Fife DA, Chen H, Slight-Webb SR, Keith MP, Harley JB, James JA. 2016. Dysregulation of innate and adaptive serum mediators precedes systemic lupus erythematosus classification and improves prognostic accuracy of autoantibodies. *Journal of Autoimmunity* **74**:182–193. DOI: <https://doi.org/10.1016/j.jaut.2016.06.001>, PMID: 27338520
- Munroe ME**, Lu R, Zhao YD, Fife DA, Robertson JM, Guthridge JM, Niewold TB, Tsokos GC, Keith MP, Harley JB, James JA. 2016. Altered type II interferon precedes autoantibody accrual and elevated type I interferon activity prior to systemic lupus erythematosus classification. *Annals of the Rheumatic Diseases* **75**:2014–2021. DOI: <https://doi.org/10.1136/annrheumdis-2015-208140>, PMID: 27088255
- Nakagawa T**, Hirano T, Nakagawa N, Yoshizaki K, Kishimoto T. 1985. Effect of recombinant IL 2 and gamma-IFN on proliferation and differentiation of human B cells. *Journal of Immunology* **134**:959–966.

- Naradikian MS**, Hao Y, Cancro MP. 2016. Age-associated B cells: key mediators of both protective and autoreactive humoral responses. *Immunological Reviews* **269**:118–129. DOI: <https://doi.org/10.1111/imr.12380>
- Nicholas MW**, Dooley MA, Hogan SL, Anolik J, Looney J, Sanz I, Clarke SH. 2008. A novel subset of memory B cells is enriched in autoreactivity and correlates with adverse outcomes in SLE. *Clinical Immunology* **126**:189–201. DOI: <https://doi.org/10.1016/j.clim.2007.10.004>, PMID: 18077220
- Obermoser G**, Pascual V. 2010. The interferon-alpha signature of systemic lupus erythematosus. *Lupus* **19**:1012–1019. DOI: <https://doi.org/10.1177/0961203310371161>, PMID: 20693194
- Pisitkun P**, Deane JA, Difilippantonio MJ, Tarasenko T, Satterthwaite AB, Bolland S. 2006. Autoreactive B cell responses to RNA-related antigens due to TLR7 gene duplication. *Science* **312**:1669–1672. DOI: <https://doi.org/10.1126/science.1124978>, PMID: 16709748
- Pollard KM**, Cauvi DM, Toomey CB, Morris KV, Kono DH. 2013. Interferon- γ and systemic autoimmunity. *Discovery Medicine* **16**:123–131. PMID: 23998448
- Portugal S**, Obeng-Adjei N, Moir S, Crompton PD, Pierce SK. 2017. Atypical memory B cells in human chronic infectious diseases: an interim report. *Cellular Immunology* **321**:18–25. DOI: <https://doi.org/10.1016/j.cellimm.2017.07.003>, PMID: 28735813
- Robinson MD**, McCarthy DJ, Smyth GK. 2010. edgeR: a bioconductor package for differential expression analysis of digital gene expression data. *Bioinformatics* **26**:139–140. DOI: <https://doi.org/10.1093/bioinformatics/btp616>, PMID: 19910308
- Rochman Y**, Spolski R, Leonard WJ. 2009. New insights into the regulation of T cells by gamma(c) family cytokines. *Nature Reviews Immunology* **9**:480–490. DOI: <https://doi.org/10.1038/nri2580>, PMID: 19543225
- Rousset F**, Garcia E, Banchereau J. 1991. Cytokine-induced proliferation and immunoglobulin production of human B lymphocytes triggered through their CD40 antigen. *Journal of Experimental Medicine* **173**:705–710. DOI: <https://doi.org/10.1084/jem.173.3.705>, PMID: 1705282
- Rubtsov AV**, Marrack P, Rubtsova K. 2017. T-bet expressing B cells - Novel target for autoimmune therapies? *Cellular Immunology* **321**:35–39. DOI: <https://doi.org/10.1016/j.cellimm.2017.04.011>, PMID: 28641866
- Rubtsova K**, Rubtsov AV, Thurman JM, Mennona JM, Kappler JW, Marrack P. 2017. B cells expressing the transcription factor T-bet drive lupus-like autoimmunity. *Journal of Clinical Investigation* **127**:1392–1404. DOI: <https://doi.org/10.1172/JCI91250>, PMID: 28240602
- Sammicheli S**, Dang VP, Ruffin N, Pham HT, Lantto R, Vivar N, Chiodi F, Rethi B. 2011. IL-7 promotes CD95-induced apoptosis in B cells via the IFN- γ /STAT1 pathway. *PLOS ONE* **6**:e28629. DOI: <https://doi.org/10.1371/journal.pone.0028629>, PMID: 22194871
- Sanz I**. 2014. Rationale for B cell targeting in SLE. *Seminars in Immunopathology* **36**:365–375. DOI: <https://doi.org/10.1007/s00281-014-0430-z>, PMID: 24763533
- Scharer CD**, Blalock EL, Barwick BG, Haines RR, Wei C, Sanz I, Boss JM. 2016. ATAC-seq on biobanked specimens defines a unique chromatin accessibility structure in naïve SLE B cells. *Scientific Reports* **6**:27030. DOI: <https://doi.org/10.1038/srep27030>, PMID: 27249108
- Scharer C**. 2019a. *genomePlots*. 04cf956. GitHub. <https://github.com/cdschar/>
- Scharer C**. 2019b. *Heatmap*. a460eca. GitHub. <https://github.com/cdschar/heatmap>
- Scharer C**. 2019c. *plotScaledBEDfeatures*. d8101e4. GitHub. <https://github.com/cdschar/plotScaledBEDfeatures>
- Shaffer AL**, Emre NC, Lamy L, Ngo VN, Wright G, Xiao W, Powell J, Dave S, Yu X, Zhao H, Zeng Y, Chen B, Epstein J, Staudt LM. 2008. IRF4 addiction in multiple myeloma. *Nature* **454**:226–231. DOI: <https://doi.org/10.1038/nature07064>, PMID: 18568025
- Sindhava VJ**, Oropallo MA, Moody K, Naradikian M, Higdon LE, Zhou L, Myles A, Green N, Nündel K, Stohl W, Schmidt AM, Cao W, Dorta-Estremera S, Kambayashi T, Marshak-Rothstein A, Cancro MP. 2017. A TLR9-dependent checkpoint governs B cell responses to DNA-containing antigens. *Journal of Clinical Investigation* **127**:1651–1663. DOI: <https://doi.org/10.1172/JCI89931>, PMID: 28346226
- Splawski JB**, Jelinek DF, Lipsky PE. 1989. Immunomodulatory role of IL-4 on the secretion of ig by human B cells. *Journal of Immunology* **142**:1569–1575.
- Stone SL**, Peel JN, Scharer CD, Risley CA, Chisolm DA, Schultz MD, Yu B, Ballesteros-Tato A, Wojciechowski W, Mousseau B, Misra RS, Hanidu A, Jiang H, Qi Z, Boss JM, Randall TD, Brodeur SR, Goldrath AW, Weinmann AS, Rosenberg AF, et al. 2019. T-bet transcription factor promotes Antibody-Secreting cell differentiation by limiting the inflammatory effects of IFN- γ on B cells. *Immunity* **50**:1172–1187. DOI: <https://doi.org/10.1016/j.immuni.2019.04.004>, PMID: 31076359
- Tangye SG**, Avery DT, Hodgkin PD. 2003. A division-linked mechanism for the rapid generation of Ig-secreting cells from human memory B cells. *The Journal of Immunology* **170**:261–269. DOI: <https://doi.org/10.4049/jimmunol.170.1.261>, PMID: 12496408
- Tangye SG**. 2015. Advances in IL-21 biology - enhancing our understanding of human disease. *Current Opinion in Immunology* **34**:107–115. DOI: <https://doi.org/10.1016/j.coi.2015.02.010>, PMID: 25801685
- Tarte K**, Zhan F, De Vos J, Klein B, Shaughnessy J. 2003. Gene expression profiling of plasma cells and plasmablasts: toward a better understanding of the late stages of B-cell differentiation. *Blood* **102**:592–600. DOI: <https://doi.org/10.1182/blood-2002-10-3161>, PMID: 12663452
- Thibault DL**, Chu AD, Graham KL, Balboni I, Lee LY, Kohlmoos C, Landrigan A, Higgins JP, Tibshirani R, Utz PJ. 2008. IRF9 and STAT1 are required for IgG autoantibody production and B cell expression of TLR7 in mice. *Journal of Clinical Investigation* **118**:1417–1426. DOI: <https://doi.org/10.1172/JCI30065>, PMID: 18340381
- Tsokos GC**, Lo MS, Costa Reis P, Sullivan KE. 2016. New insights into the immunopathogenesis of systemic lupus erythematosus. *Nature Reviews Rheumatology* **12**:716–730. DOI: <https://doi.org/10.1038/nrrheum.2016.186>, PMID: 27872476

- Wang S**, Wang J, Kumar V, Karnell JL, Naiman B, Gross PS, Rahman S, Zerrouki K, Hanna R, Morehouse C, Holoweckyj N, Liu H, Manna Z, Goldbach-Mansky R, Hasni S, Siegel R, Sanjuan M, Streicher K, Cancro MP, Kolbeck R, et al. 2018. IL-21 drives expansion and plasma cell differentiation of autoreactive CD11chiT-bet⁺ B cells in SLE. *Nature Communications* **9**:9. DOI: <https://doi.org/10.1038/s41467-018-03750-7>
- Wei C**, Anolik J, Cappione A, Zheng B, Pugh-Bernard A, Brooks J, Lee EH, Milner EC, Sanz I. 2007. A new population of cells lacking expression of CD27 represents a notable component of the B cell memory compartment in systemic lupus erythematosus. *The Journal of Immunology* **178**:6624–6633. DOI: <https://doi.org/10.4049/jimmunol.178.10.6624>, PMID: 17475894
- Welcher AA**, Boedigheimer M, Kivitz AJ, Amoura Z, Buyon J, Rudinskaya A, Latinis K, Chiu K, Oliner KS, Damore MA, Arnold GE, Sohn W, Chirmule N, Goyal L, Banfield C, Chung JB. 2015. Blockade of interferon- γ normalizes interferon-regulated gene expression and serum CXCL10 levels in patients with systemic lupus erythematosus. *Arthritis & Rheumatology* **67**:2713–2722. DOI: <https://doi.org/10.1002/art.39248>, PMID: 26138472
- Zhang Y**, Liu T, Meyer CA, Eeckhoutte J, Johnson DS, Bernstein BE, Nusbaum C, Myers RM, Brown M, Li W, Liu XS. 2008. Model-based analysis of ChIP-Seq (MACS). *Genome Biology* **9**:R137. DOI: <https://doi.org/10.1186/gb-2008-9-9-r137>, PMID: 18798982
- Zhu J**, Yamane H, Paul WE. 2010. Differentiation of effector CD4 T cell populations (*). *Annual Review of Immunology* **28**:445–489. DOI: <https://doi.org/10.1146/annurev-immunol-030409-101212>, PMID: 20192806